

USING VEHICLE DYNAMICS SIMULATION AND METAMODELS TO EVALUATE
FACTORS AND MECHANISMS AFFECTING ROLL ANGLE: AN INITIAL ASSESSMENT

A Thesis

by

MELISSA MARISOL MARTINEZ

Submitted to the Office of Graduate and Professional Studies of
Texas A&M University
in partial fulfillment of the requirements for the degree of

MASTER OF SCIENCE

Chair of Committee, Gary Fry
Committee Members, Nasir Gharaibeh
Alan Palazzolo

Head of Department, Robin Autinreth

May 2018

Major Subject: Civil Engineering

Copyright 2018 Melissa Marisol Martinez

ABSTRACT

A rollover is defined as any vehicle rotation of 90 degrees or more about a longitudinal or lateral axis, according to NASS CDS. Rollover crashes are still represented highly in terms of frequency and fatalities when compared to other crash categories. Even though there are various vehicular technical innovations that act as a preventative or protective improvement, rollover crashes and subsequent loss of life and injuries are still prevalent in crash statistics. In 2015, rollovers represented 33% of occupant fatalities. Existing research on rollover as it relates to highway safety is often based on crash data analysis. Limited studies have investigated the initiating mechanisms contributing to vehicular propensity to rollover. Hence, there is a gap in knowledge to understand initiation factors that affect rollover events. Herein, vehicle dynamics simulations will be utilized to examine several vehicle rollover crash scenarios. A second aspect of this research is to develop a metamodel of vehicle roll angle as a function of initiation/influencing factors. A total of 282 vehicle rollover scenarios were created and data from the simulations was used to build metamodels. The vehicle rollover scenarios were split up into 16 categories. The surface metamodel, accuracy model, and global sensitivities were analyzed. These models show that for all the categories, speed had the greatest influence on the vehicle's propensity to roll over. Friction held a greater influence on the deviation from the centerline of the right lane.

ACKNOWLEDGEMENTS

I would like to thank my committee chair, Dr. Fry, and my committee members, Dr. Gharaibeh and Dr. Palazzolo, for their guidance and support throughout this process. I would also like to thank Dr. Abu-Odeh and Maryam Tavakoli for their guidance this past year.

I would also like to thank my colleagues and friends at Texas A&M University and Texas A&M Transportation Institute for making my time in College Station an enjoyable experience. Graduate school would not have been as fun without you guys! Nataly, you have been the best of friends and going through graduate school has been an incredible experience.

Eloy, thank you for moving six hours away from family to help me pursue my graduate degree. This experience has been wonderful with you by my side. To my parents, thank you for always allowing and encouraging me to pursue my dreams. I owe all my success to you.

CONTRIBUTORS AND FUNDING SOURCES

Contributors

This work was supervised by a thesis committee consisting of Dr. Gary Fry, Dr. Nasir Gharaibeh of the Zachary Department of Civil Engineering and Dr. Alan Palazzolo of the Department of Mechanical Engineering.

All work for the thesis was completed by the student, in collaboration with Dr. Akram Abu-Odeh of the Texas A&M Transportation Institute.

Funding Sources

This work was made possible in part by Advancing Transportation Leadership and Safety under Project Number 602761.

TABLE OF CONTENTS

	Page
ABSTRACT	ii
ACKNOWLEDGEMENTS	iii
TABLE OF CONTENTS	v
LIST OF FIGURES	vii
LIST OF TABLES	xi
INTRODUCTION	1
Motivation	1
Research Objectives	4
BACKGROUND INFORMATION	5
Fundamentals Of Vehicle Dynamics	5
Driver Behavior	13
Vehicle Dynamics Code	14
Metamodeling Software	15
PROCEDURES	19
Vehicle Dynamics Simulations	19
Metamodeling	20
RESULTS	22
Vehicle Dynamics Simulation Results	22
Metamodeling Results	22
Full Size SUV Metamodels	22
Class C Hatchback Metamodels	23

DISCUSSION.....	25
CONCLUSIONS	27
REFERENCES	29
Supplemental Sources Consulted.....	30
APPENDIX A.....	33
APPENDIX B.....	37

LIST OF FIGURES

	Page
FIGURE 1. CARSIM SIMULATION FLOWCHART	37
FIGURE 2. CARSIM RUN CONTROL SCREEN	38
FIGURE 3 CARSIM PROCEDURES SCREEN.....	38
FIGURE 4 CLASS C HATCHBACK	39
FIGURE 5 FULL-SIZE SUV	39
FIGURE 6 621.79 METER RADIUS ROAD WITH A 3:1 SIDE-SLOPE	40
FIGURE 7. STRAIGHT ROAD WITH A 3:1 SIDE-SLOPE	40
FIGURE 8. ROAD PROFILE OF THE 3:1 SIDE-SLOPE	41
FIGURE 9. ROAD PROFILE OF 4:1 SIDE-SLOPE.....	41
FIGURE 10. LS-OPT USER INTERFACE	42
FIGURE 11 LS-OPT CATEGORIES	42
FIGURE 12. SURFACE METAMODEL AND GLOBAL SENSITIVITY ANALYSIS: SUV, 3:1 CURVED ROAD, 15 DEGREE ENCROACHMENT ANGLE.....	43
FIGURE 13. SURFACE METAMODEL AND GLOBAL SENSITIVITY ANALYSIS: SUV, 3:1 CURVED ROAD, 25 DEGREE ENCROACHMENT ANGLE.....	44
FIGURE 14. SURFACE METAMODEL AND GLOBAL SENSITIVITY ANALYSIS: SUV, 3:1 STRAIGHT, 15 DEGREE ENCROACHMENT ANGLE	45
FIGURE 15. SURFACE METAMODEL AND GLOBAL SENSITIVITY ANALYSIS: SUV, 3:1 STRAIGHT ROAD, 25 DEGREE ENCROACHMENT ANGLE.....	46
FIGURE 16. SURFACE METAMODEL AND GLOBAL SENSITIVITY ANALYSIS: SUV, 4:1 CURVED, 15 DEGREE ENCROACHMENT ANGLE.	47

FIGURE 17. SURFACE METAMODEL AND GLOBAL SENSITIVITY ANALYSIS: SUV, 4:1 CURVED ROAD, 25 DEGREE ENCROACHMENT ANGLE.....	48
FIGURE 18. SURFACE METAMODEL AND GLOBAL SENSITIVITY ANALYSIS: SUV, 4:1 STRAIGHT ROAD, 15 DEGREE ENCROACHMENT ANGLE.....	49
FIGURE 19. SURFACE METAMODEL AND GLOBAL SENSITIVITY ANALYSIS: SUV, 4:1 STRAIGHT ROAD, 25 DEGREE ENCROACHMENT ANGLE.....	50
FIGURE 20. SURFACE METAMODEL AND GLOBAL SENSITIVITY ANALYSIS: SUV, 3:1 CURVED ROAD, 15 DEGREE ENCROACHMENT ANGLE.....	51
FIGURE 21. SURFACE METAMODEL AND GLOBAL SENSITIVITY ANALYSIS: SUV, 3:1 CURVED ROAD, 25 DEGREE ENCROACHMENT ANGLE.....	52
FIGURE 22. SURFACE METAMODEL AND GLOBAL SENSITIVITY ANALYSIS: SUV, 3:1 STRAIGHT ROAD, 15 DEGREE ENCROACHMENT ANGLE.....	53
FIGURE 23. SURFACE METAMODEL AND GLOBAL SENSITIVITY ANALYSIS: SUV, 3:1 STRAIGHT ROAD, 25 DEGREE ENCROACHMENT ANGLE.....	54
FIGURE 24. SURFACE METAMODEL AND GLOBAL SENSITIVITY ANALYSIS: SUV, 4:1 CURVED ROAD, 15 DEGREE ENCROACHMENT ANGLE.....	55
FIGURE 25. SURFACE METAMODEL AND GLOBAL SENSITIVITY ANALYSIS: SUV, 4:1 CURVED ROAD, 25 DEGREE ENCROACHMENT ANGLE.....	56
FIGURE 26. SURFACE METAMODEL AND GLOBAL SENSITIVITY ANALYSIS: SUV, 4:1 STRAIGHT ROAD, 15 DEGREE ENCROACHMENT ANGLE.....	57
FIGURE 27. SURFACE METAMODEL AND GLOBAL SENSITIVITY ANALYSIS: SUV, 4:1 STRAIGHT ROAD, 25 DEGREE ENCROACHMENT ANGLE.....	58

FIGURE 28. SURFACE METAMODEL AND GLOBAL SENSITIVITY ANALYSIS: CLASS C HATCHBACK, 3:1 CURVED ROAD, 15 DEGREE ENCROACHMENT ANGLE.	59
FIGURE 29. SURFACE METAMODEL AND GLOBAL SENSITIVITY ANALYSIS: CLASS C HATCHBACK, 3:1 CURVED ROAD, 25 DEGREE ENCROACHMENT ANGLE.	60
FIGURE 30 SURFACE METAMODEL AND GLOBAL SENSITIVITY ANALYSIS: CLASS C HATCHBACK, 3:1 STRAIGHT ROAD, 15 DEGREE ENCROACHMENT ANGLE.	61
FIGURE 31 SURFACE METAMODEL AND GLOBAL SENSITIVITY ANALYSIS: CLASS C HATCHBACK, 3:1 STRAIGHT ROAD, 25 DEGREE ENCROACHMENT ANGLE.	62
FIGURE 32 SURFACE METAMODEL AND GLOBAL SENSITIVITY ANALYSIS: CLASS C HATCHBACK, 4:1 CURVED ROAD, 15 DEGREE ENCROACHMENT ANGLE.	63
FIGURE 33 SURFACE METAMODEL AND GLOBAL SENSITIVITY ANALYSIS: CLASS C HATCHBACK, 4:1 CURVED ROAD, 25 DEGREE ENCROACHMENT ANGLE.	64
FIGURE 34 SURFACE METAMODEL AND GLOBAL SENSITIVITY ANALYSIS: CLASS C HATCHBACK, 4:1 STRAIGHT ROAD, 15 DEGREE ENCROACHMENT ANGLE.	65
FIGURE 35 SURFACE METAMODEL AND GLOBAL SENSITIVITY ANALYSIS: CLASS C HATCHBACK, 4:1 STRAIGHT ROAD, 25 DEGREE ENCROACHMENT ANGLE.	66
FIGURE 36 SURFACE METAMODEL AND GLOBAL SENSITIVITY ANALYSIS: CLASS C HATCHBACK, 3:1 CURVED ROAD, 15 DEGREE ENCROACHMENT ANGLE	67
FIGURE 37 SURFACE METAMODEL AND GLOBAL SENSITIVITY ANALYSIS: CLASS C HATCHBACK, 3:1 CURVED ROAD, 25 DEGREE ENCROACHMENT ANGLE	68
FIGURE 38 SURFACE METAMODEL AND GLOBAL SENSITIVITY ANALYSIS: CLASS C HATCHBACK. 3:1 STRAIGHT ROAD, 15 DEGREE ENCROACHMENT ANGLE	69

FIGURE 39 SURFACE METAMODEL AND GLOBAL SENSITIVITY ANALYSIS: CLASS C HATCHBACK, 3:1	
STRAIGHT ROAD, 25 DEGREE ENCROACHMENT ANGLE	70
FIGURE 40 SURFACE METAMODEL AND GLOBAL SENSITIVITY ANALYSIS: CLASS C HATCHBACK, 4:1	
CURVED ROAD, 15 DEGREE ENCROACHMENT ANGLE	71
FIGURE 41 SURFACE METAMODEL AND GLOBAL SENSITIVITY ANALYSIS: CLASS C HATCHBACK, 4:1	
CURVED ROAD, 25 DEGREE ENCROACHMENT ANGLE	72
FIGURE 42 SURFACE METAMODEL AND GLOBAL SENSITIVITY ANALYSIS: CLASS C HATCHBACK, 4:1	
STRAIGHT ROAD, 15 DEGREE ENCROACHMENT ANGLE	73
FIGURE 43 SURFACE METAMODEL AND GLOBAL SENSITIVITY ANALYSIS: CLASS C HATCHBACK, 4:1	
STRAIGHT ROAD, 25 DEGREE ENCROACHMENT ANGLE	74

LIST OF TABLES

	Page
TABLE 1. TEXAS FATALITIES BY CRASH TYPE	33
TABLE 2. PASSENGER VEHICLE OCCUPANT DEATHS IN SINGLE-VEHICLE ROLLOVER CRASHES, 1978- 2015.....	33
TABLE 3. DEATHS IN SINGLE-VEHICLE CRASHED AS A PERCENT OF ALL OCCUPANT DEATHS, 2015	34
TABLE 4. PASSENGER VEHICLE OCCUPANT DEATHS IN ROLLOVER VS. NO ROLLOVER CRASHES, 1978-2015	35
TABLE 5. CENTER OF GRAVITY HEIGHT, ROLLOVER THRESHOLD.....	36
TABLE 6. VEHICLE DYNAMICS SIMULATION MATRIX.....	36

INTRODUCTION

Motivation

The rollover crash is one of the most fatal forms of crashes among passenger vehicles. These types of crashes account for 33% of all occupant fatalities in 2015. Table 1 summarizes crash data from 2012 to 2016 for the state of Texas. In 2015, there were a total of 32,166 fatal crashes in the US. Of these 32,166 crashes, there were a total of 35,092 fatalities. 48% of these crashes occurred in rural areas, 45% occurred in urban areas and 8% of the crashes happened in unknown areas [1]. 38% of rural crashes involved vehicle rollovers and 24% of rollover crashes happened in urban areas. The percentage of fatalities in rollover crashes was highest for SUVs (36%), followed by pickup trucks (30%), vans (22%), and passenger cars (20%) [1]. Fatal crashes have declined by 16.8% over the past decade, but have increased by 7% in the last year. Fatality rate per 100 million vehicle miles traveled was 2.6 times higher in rural areas than in urban areas. Table 2 shows the passenger vehicle occupant deaths in single-vehicle rollover crashes [2]. Occupant deaths have fluctuated over the years. Deaths in car drivers has had an overall decrease since 1978 while deaths in SUV drivers has increased significantly since then. Although much research has been done on the topic, there is still a gap in knowledge to understand initiation factors that affect rollover events. Many factors contribute to a vehicle's roll angle. Vehicle type, vehicle center of gravity, speed, roadway characteristics, and driving behaviors are just a few that influence a vehicle's roll angle.

The type of vehicle and its corresponding center of gravity greatly influence the vehicle's propensity to rollover. A vehicle with a low center of gravity (CG) is less likely to topple over than one with a higher CG. So, a Full-size SUV is more likely to roll over than a sedan since the

SUV has a higher center of gravity than the sedan. Table 3 shows deaths in single-vehicle crashed as a percent of all occupant deaths in 2015 [3]. The largest percentage in single-vehicle rollovers were large SUVs'. For this reason, the SUV was chosen as one of the vehicle types studied. The primary goal of roadside design is to limit the amount of serious injuries and fatalities associated with ran-off road crashes. Roadside geometrics and safety features have a strong influence on the severity and frequency of crashes. To design optimum roadside geometrics and to determine which roadside safety features are adequate, it is vital to identify impact characteristics associated with serious injury and fatal crashes. It is important to have definitive data on whether there are real relationships between the selected test impact conditions and actual crashes involving serious injuries and fatalities. The safety performance of roadside features is evaluated primarily through full-scale crash testing. Testing is used to observe and evaluate the performance of safety features under impact conditions that are either similar or more severe than those associated with real world crashes resulting in serious injuries or fatalities. Even though full scale crash test data provides a small window into the nature of ran-off road crashes, it does not provide sufficient data to identify the impact conditions associated with serious injury and fatal crashes. American Association of State Highway and Transportation Officials (AASHTO) current policy states that shoulder slopes that drain away from the paved surface on the outside of a super-elevated horizontal curve should be designed to avoid too great a cross-slope break, calculated as the algebraic difference between the cross-slope of the traveled way and shoulder [4]. To avoid large pavement/shoulder cross-slope breaks, it may be desirable that all or part of the shoulder be sloped upward at about the same or lesser that the super-elevated traveled way. The Roadside Design Guide [5] indicates the roadside should be rounded

because it reduces the chances of an errant vehicle becoming airborne. This also affords the driver more control over the vehicle. A superelevation of 6% was assumed for this study.

Side-slopes and ditches have been identified as the primary tripping mechanism in single vehicle ran-off-road (SVROR) rollovers [6]. Side-slopes refer to the slopes of areas adjacent to the shoulder and located between the shoulder and the right-of-way line, according to TxDOT. A relatively flat area adjacent to the travel-way is desired so that out-of-control vehicles are less likely to turn over, vault, or impact the side of a drainage channel. Steeper slope ratios (3:1) are negotiable by drivers. However, recovery on these steeper slopes is less likely. Where conditions are favorable, it is desirable to use flatter slopes to increase roadside safety. The front slope is the slope adjacent to the shoulder. The front slope should be 6:1 or flatter. Slope rates of 3:1 may be used in constrained conditions. Since recovery is less likely on 3:1 and 4:1 slopes, fixed objects should not be present in the vicinity of the toe of the slopes. The intersections of slope planes in the highway cross section should be well rounded for added safety, increased stability, and improved aesthetics. Two slopes were considered for this study; 3:1 and 4:1 slopes. Slopes were purposely made long to understand how the slope and not the ditch affected a vehicle's roll angle.

Using the vehicle dynamics code, CarSim, several vehicle rollover scenarios were created to assess how roadway characteristics and driver inputs affect the vehicle's roll angle. Data from CarSim will be input into LS-OPT to create different metamodels. Metamodeling is the analysis, construction, and development of the frame, rules, constraints, models, and theories applicable and useful for modeling a predefined class of problems. A metamodel of vehicle roll angle as a function of speed, friction, curvature, encroachment angle, and ditch slope is to be developed and discussed.

Research Objectives

The objective of this research is to:

1. Enhance our understanding of rollover propensity giving certain roadway designs, vehicle types, vehicle speed and and maneuvers.
2. To use vehicle dynamics simulations to examine several vehicle rollover crash scenarios.

BACKGROUND INFORMATION

Fundamentals of vehicle dynamics

The first practical automobiles that were powered by gasoline engines came in 1886 by Karl Benz and Gottlieb Daimler. Over the following decade, automotive vehicles were developed by others pioneers with familiar names such as Henry Ford and Ransom Olds. By 1908 the automotive industry was well established in the United States of America with Henry Ford manufacturing the Model T. The General Motors Corporation was also founded around this time. By 1909, over 600 makes of American cars had been identified [7].

In the early 1900s, most of the engineering in the automotive industry went into invention and design that would yield faster, more comfortable, and more reliable vehicles. In general, motor vehicles achieved high speed capability well before good paved roads existed on which to use them. With higher speeds the dynamics of vehicles assumed greater importance as an engineering concern. One of the first engineers to write on automotive dynamics was Frederick William Lanchester. Steering shimmy problems were prevalent at that time as well. The understanding of both turning behavior and the shimmy problems was hampered by a lack of knowledge about tire mechanics in these early years. In 1931, a test device was built which could measure the necessary mechanical properties of the pneumatic tire for the understandings to be developed. Only then could engineers develop mechanistic explanations of the turning behavior of automobiles which lays the groundwork for much of our understanding today. Engineers have achieved dramatic advancements in the technologies employed in automobiles from the Model t to the Taurus. More than ever, dynamics plays an important role in vehicle design and development.

A knowledge of the forces and moments generated by pneumatic rubber tires at the ground is essential to understanding highway vehicle dynamics. The motions accomplished in accelerating, braking, cornering, and ride is a response to forces imposed. The dominant forces acting on a vehicle to control performance are developed by the tire against the road. Therefore, it becomes necessary to develop an understanding of the behavior of tires, characterized by the forces and moments generated over the broad range of conditions over which they operate.

Understanding vehicle dynamics can be accomplished at two levels; the empirical and the analytical. The empirical understanding derives from trial and error by which one learns which factors influence vehicle performance, in which way, and under what conditions. However, the empirical method can often lead to failure. Without mechanistic understanding of how changes in vehicle design or properties affect performance, extrapolating past experience to new conditions may involve unknown factors which may produce a new result, defying the prevailing rules of thumb. For this reason, engineers favor an analytical approach. The analytical approach attempts to describe the mechanics of interest based on the known laws of physics so that an analytical model can be established. In the more simple cases the models can be represented by algebraic or differential equations that relate forces or motions of interest to control inputs and vehicle or tire properties. These equations then allow one to evaluate the role of each vehicle property. The existence of the model thereby provides a means to identify the important factors, the way in which they operate and under which conditions. It should be noted that the analytical methods also are not foolproof because they usually only approximate reality.

Before, many of the shortcomings of analytical methods were a consequence of the mathematical limitations in solving problems. Before computers, analysis was only considered successful if the problem could be reduced to a closed form solution. This limited the

functionality of the analytical approach to solution of problems in vehicle dynamics. The existence of large numbers of components, systems, sub-systems, and nonlinearities in vehicles made comprehensive modeling virtually impossible, and the only utility obtained came from rather simplistic models of certain mechanical systems. The simplicity of the models can often constituted deficiencies that handicapped the engineering approach in vehicle development. Now, with the computational power, a major shortcoming of the analytical method has been overcome. It is now possible to assemble models for the behavior of individual components of a vehicle, allowing simulation and evaluation of its behavior before being rendered in hardware. These models can calculate performance that could not be solved for in the past. In cases where the engineer is uncertain of the importance of specific properties, those properties can be included in the model and their importance assessed by evaluating their influence on simulated behavior. This provides the engineer with a new tool as a means to test our understanding of a complex systems and investigate means of improving performance.

The subject of vehicle dynamics is concerned with the movements of vehicles on a road surface. The movements of interest are acceleration and braking, ride, and turning. Dynamic behavior is determined by the forces imposed on the vehicle from the tires, gravity, and aerodynamics. The vehicle and its components are studied to determine what forces will be produced by each of these sources at a particular maneuver and trim condition, and how the vehicle will respond to these forces. It is essential to establish an approach to modeling the systems and the conventions that will be used to describe motions.

A motor vehicle is made up of many components distributed within its exterior envelope. For many of the elementary analysis applied to it, all components move together. Under braking, the entire vehicle slows down as a unit. Thus, it can be represented as one lumped mass located

at its center of gravity. For acceleration, braking, and most turning analysis, one mass is sufficient. For single mass representation, the vehicle is treated as a mass concentrated at its center of gravity (CG). The point mass at the CG, with appropriate rotational moments of inertia, is dynamically equivalent to the vehicle itself for all motions in which it is reasonable to assume the vehicle to be rigid.

The vehicle motions are defined with reference to a right-hand orthogonal coordinate system which originates at the CG and travels with the vehicle, as follows:

- X= forward and on the longitudinal plane of symmetry
- Y= lateral out the right side of the vehicle
- Z= downward with respect to the vehicle
- P= roll velocity about the x-axis
- Q= pitch velocity about the y-axis
- R= yaw velocity about the z-axis.

Vehicle motion is usually described by the velocities with respect to the vehicle fixed coordinate system, where the velocities are reference to the earth fixed coordinate system.

Vehicle attitude and trajectory through the course of a maneuver are defined with respect to a right-hand orthogonal axis system fixed on the earth. The coordinates are:

- X- forward travel
- Y- travel to the right
- Z- vertical travel (Positive downward)
- Ψ - heading angle (the angle between x and X in the ground)

- γ - Course angle (the angle between the vehicle's velocity vector and X-axis)
- β - sideslip angle (the angle between x-axis and the vehicle velocity vector)

Forces and moments are normally defined as they act on the vehicle. A positive force in the longitudinal direction on the vehicle is forward. The force corresponding to the load on the tire acts in the upward direction and is therefore negative in magnitude. The SAE J670e "vehicle dynamics terminology" gives the name normal force as that acting downward and the vertical force as the negative of the normal forces. Therefore, the vertical force is the equivalent of the tire load with a positive convention in the upward direction.

The fundamental law from which most vehicle dynamics analysis begin is the second law formulated by Sir Isaac Newton. The law applies to both translational and rotational systems. Translational systems are the sum of the external forces acting on a body in a given direction is equal to the product of its mass and the acceleration in that direction (assuming the mass is fixed).

$$\sum F_x = M * a_x \quad (1)$$

where:

- F_x = Forces in the x-direction
- M = Mass of the body
- A_x = Acceleration in the x-direction

Rotational systems are the sum of the torques acting on a body about a given axis is equal to the product of its rotational moment of inertia and the rotational acceleration about that axis

$$\sum T_x = I_{xx} * \alpha_x \quad (2)$$

where:

- T_{xx} = Torques about the x-axis
- I_{xx} = Moment of inertia about the x-axis
- α_x = Rotational Acceleration about the x-axis

Determining the axle loading on a vehicle under arbitrary conditions is an application of Newton's Second Law.

W is the weight of the vehicle acting at its CG with a magnitude equal to its mass times the acceleration of gravity. If the vehicle is accelerating along the road it is convenient to represent the effect by an equivalent inertial force known as a "d'Alembert force" acting at the center of gravity opposite to the direction of the road. The tires will experience a force normal to the road representing the dynamic weights carried on the front and rear wheels. Tractive forces or rolling resistance forces may act in the ground plane in the tire contact patch. D_A is the aerodynamic force acting on the body of the vehicle. It may be represented as acting at a point above the ground indicated by the height or by a longitudinal force of the same magnitude in the ground with an associated moment equivalent to D_A times h_A .

The influence of grade on axle loads is also worth considering. Grade is defined as the rise over the run. The ratio is equal to the tangent of the grade angle. Common grades on interstate highways are limited to 4 percent wherever possible. Primary and secondary roads occasionally reach 10 to 12 percent grades.

Amongst the dynamic maneuvers a vehicle can experience, rollover is one of the most serious and threatening to the occupants. Rollover may be defined as any maneuver in which the vehicle rotates 90 degrees or more about its longitudinal axis such that the body makes contact with the ground. Rollover may be precipitated from one or more combination of factors. It may

occur on flat and level surfaces when the lateral accelerations on a vehicle reach a level beyond that which can be compensated by lateral weight shift on the tires. Cross-slope of the road surface may contribute along with disturbances to the lateral forces arising from curb impacts, soft ground, or other obstructions that may trip the vehicle. The vehicle rollover is one that involves a complex interaction of forces acting on and within the vehicle. The forces are influenced by the maneuver and roadway. This process has been investigated analytically and empirically using models that cover a range of complexities. The rollover process is most easily understood by starting with the fundamental mechanics involved in a quasi-static case and progressing to the more complex models.

The most basic mechanics involved in rollovers can be seen by considering the balance of forces on a rigid vehicle in cornering. In a cornering maneuver the lateral forces act in the ground plane to counterbalance the lateral acceleration acting at the CG of the vehicle. The difference in the position at which these forces act creates a moment on the vehicle which attempts to roll toward the outside of the turn. Taking moments about the center of contact for the outside tires yields:

$$\frac{a_y}{g} = \frac{\frac{t}{2} + \varphi h - \frac{F_z i_t}{Mg}}{h} \quad (3)$$

On a level road, $\varphi = 0$ with no lateral acceleration.

In a highway design, cross-slope is used in curves exactly for this purpose. Given the radius of turn and an intended travel speed, the cross-slope will be chosen to produce a lateral acceleration in the range of zero to 0.1 g's. As the lateral acceleration builds up, the load on the inside wheels must diminish. Through this process the vehicle acts to resist or counterbalance the roll moment in cornering. The limit cornering condition will occur when the load on the inside wheels reaches zero. At that point, rollover will begin because the vehicle can no longer maintain

equilibrium in the roll plane. The lateral acceleration at which rollover begins is the rollover threshold and is given by:

$$\frac{a_y}{g} = \frac{t + \phi h}{h} \quad (4)$$

With no cross-slope the lateral acceleration that constitutes the rollover threshold is

$$\frac{a_y}{g} = \frac{t}{2h} \quad (5)$$

This value is also known as the static stability factor or SSF [8]. The rollover threshold differs amongst the various types of vehicles on the road. Typical values fall in the following ranges listed in Table 5.

The rigid-vehicle model suggests that the lateral acceleration necessary to reach the rollover of passenger cars and light trucks exceeds the cornering capabilities arising from the friction limits of the tires. It is possible for a car to spin out on a flat surface without rolling over. From this, one may conclude that rollover with these kinds of vehicles should be rare. However, accident statistics prove otherwise. This motivates a more in depth analysis of rollover phenomenon. In the case of heavy trucks, it is possible to reach the rollover threshold within the friction limits of the tires.

Rigid body rollover can be illustrated by plotting the lateral acceleration as a function of roll angle for the equilibrium of the vehicle. While at a zero roll angle, the lateral acceleration can be any value up to the rollover threshold. Once this threshold is reached, the inside of the wheel will lift. The vehicle then begins to roll and the equilibrium lateral acceleration decreases with angle because the center of gravity is lifting and shifting toward the outside of the wheels. Consider a vehicle tipped on two wheels in a turn. The vehicle roll angle must be at the precise value where the equilibrium lateral acceleration matches the actual lateral acceleration in order to

be in equilibrium. A reduction of the equilibrium lateral acceleration can be caused by a slight disturbance that increases the roll angle. The excess lateral acceleration produces a roll acceleration that further increases that angle driving away from the equilibrium point. If this continues, the vehicle roll attitude accelerated rapidly to complete the rollover in a matter of a second or two.

It is appropriate to consider wheel lift-off as the beginning of rollover because of the inherent instability of the vehicle when the inside wheels leave the ground. However, it is possible for a driver to halt the action by quickly steering out of the turn, thereby reducing the lateral acceleration to a level that will return the vehicle to an upright position. A fast response is necessary because of the speed with which rollover proceeds. Rollover becomes irreversible only when the roll angle becomes so large that the center of gravity of the vehicle passes outboard of the line of contact of the outside wheels. The limit corresponds to the point in the graph where the equilibrium lateral acceleration reaches zero. Stunt drivers can take a vehicle up to this point and drive on two wheels for extended distances despite the instability. But, it is a rare event for a typical motorist to avoid rollover if the vehicle should inadvertently roll to this position.

Driver Behavior

In 1977, the Society of Automotive Engineers conducted a study in which they observed a sedan traveling at 60 km/hr faced with an emergency that is 1.3 seconds to collision. The severity of the emergency forced the driver to perform an emergency maneuver without braking. During the test, the drivers were told to avoid the emergency by performing a lane change through a 3.66 meter lateral displacement. The common maximum steering angle of all the drivers was between 210 and 230 degrees. Although the Society of Automotive Engineers' study

was a useful reference, it did not provide guidance for the behavior of a driver returning to the travel lane. Braking was not applied during emergency avoidance situations [9].

With the use of a Computer Assisted Virtual Environment driving simulator, Kim et al. recorded driver response to an emergency that is 1.3 seconds to collision [10]. The driving simulator tested a sedan at 50 km/hr driving behind a truck that suddenly stops. The simulation maneuver occurred on a straight urban road with a friction coefficient of 0.8. The braking was determined to be zero due to the severity of the emergency and the necessity for avoidance rather than stopping. This simulation scenario included data for the vehicle to return to the travel lane.

Vehicle Dynamics Code

Vehicle dynamics models serve a variety of purposes on simulations [11]. A model must have sufficient complexity for the given application but should not be too complicated. In stability and handling simulations, various modes must be properly represented, including lateral/directional and longitudinal degrees of freedom. Limit performance effects of tire saturation that lead to plow out, spin out, and skidding require adequate tire force response models. Steering and braking subsystem characterization are necessary to represent important handling and stability requirements. A comprehensive set of vehicle dynamics model elements are listed below.

- The basic inertial vehicle dynamics, including the interaction of sprung and unsprung masses and the wheel spin modes
- A comprehensive tire model that includes lateral and longitudinal force response to normal load, slip, and camber

- Power train including engine torque production and transmission and drive train components for transmitting the torque to the drive wheels
- Steering system with power assist characteristics and compliance that produces understeer
- Braking system including proportioning and antilock characteristics to minimize rear wheel lock up
- Vehicle/ road kinematics that compute vehicle position and orientation relative to the roadway and terrain
- A driver or automatic controller for steering, throttle, and brake control
- External forces and commands that produce system responses through vehicle motions and driver or automatic system control.

CarSim is a vehicle dynamics code that provides physical predictions of vehicle dynamical behavior in a form that can be used by most engineers and technical staff. It includes graphic user interface, database management, animation, and plotting.

Metamodeling Software

LS-OPT is a standalone design optimization and probabilistic analysis package that can be linked with several analyses programs or datasets of results of simulations or tests outcomes [12]. LS-OPT allows the user to structure the design process, explore the design space, and compute optimal designs according to specified constraints and objectives. In the design approach, a design is improved by evaluating its response and making design changes based on experience or intuition. This approach does not always lead to the desired result since the design objectives are often in conflict. Therefore, it is not always clear how to change the design to

achieve the best compromise of these objectives. A systematic approach can be obtained by using an inverse process of first specifying the criteria and then computing the best design according to a formulation. The improvement procedure that incorporates these design criteria into a mathematical framework is referred to as design optimization. This procedure is iterative and requires multiple simulations. Response surface methodology is a statistical method for constructing smooth approximations to functions in a multi-dimensional space. It is a methodology to address optimization. Response surface methodology selects designs that are optimally distributed throughout the design space to construct the approximate surfaces. To check the adequacy of the model, the equation for the residual sum of squares formula is used. The metrics used for the quality of these surfaces are the RMS error and the coefficient of determination R^2 . The surface level of accuracy is improved with R^2 is valued at 1 or very close to 1 and RMS error is very small or closer to zero. Practical values are dependent on the problem at hand and the desired accuracy. The coefficient of determination R^2 , and the RMS error values are calculated using the equations below.

$$R^2 = \frac{\sum_{i=1}^P (\hat{y}_i - \bar{y})^2}{\sum_{i=1}^P (y_i - \bar{y})^2} \quad (6)$$

$$\varepsilon_{RMS} = \sqrt{\frac{1}{P} \sum_{i=1}^P (y_i - \hat{y}_i)^2} \quad (7)$$

where:

P: number of design points

Y: predicted response

Y_i : mean of the responses

Y_i : the actual response

Two sensitivity measures are implemented in LS-OPT: Linear ANOVA and GSA/Sobol. If a polynomial response surface method is selected, the analysis of variance (ANOVA) of the approximation to the experimental design is automatically performed. The ANOVA information can be used to screen variables during or at the start of the optimization process. The ANOVA method determines the significance of main and interaction effects. The ANOVA results are viewed in a bar/tornado chart form. The ANOVA bars show which design variable is important for the computation of the response. Figure 4 shows ANOVA calculations. The ANOVA value is represented by the blue bar. The red bar indicates the confidence interval. When a red bar is too large, the value computed cannot be trusted. When the red bar is small, the confidence interval is small and the contribution of that variable is substantial. In this figure the speed held the most substantial contribution. A global sensitivity analysis (GSA) is to be performed as well. Each bar represents a variable and its contribution of the variable to the variance of the respective response. The values sum to 100%. The variance of the response may be written using the Sobol's indices approach.

$$f(x_1, \dots, x_n) = f_0 + \sum_{i=1}^n f_i(x_i) + \sum_{i=1}^n \sum_{j=i+1}^n f_{ij}(x_i, x_j) + \dots + f_{1,2,\dots,n}(x_1, \dots, x_n) \quad (8)$$

Neural networks can be divided into three basic categories: feed-forward, feed-back, and self-organizing [13]. Each category is based on a different philosophy and obeys different principles, the characterization of a system by the term “neural network” implies an ability to learn. Feed-forward neural networks contain one or more layers of nonlinear processing elements or units. The elements belonging to neighboring layers are connected by sets of synaptic weights.

These neural architectures are called feed-forward since the output of each layer feeds the next layer of elements. The Perceptron and the Adaline are the earliest feed-forward neural architectures. Multi-layered neural networks include one or more layers of hidden elements between the input and output layer. The feed-forward neural network may be seen as a system transforming a set of input patterns into a set of output patterns. This type of neural network can be trained to provide a desired response to a given input. The network achieves this by adapting its synaptic weights during the learning phase on the basis of learning rules. The training of feed-forward neural networks requires the existence of a set of input and output patterns. This type of learning is called supervised learning.

PROCEDURES

Through simulation, combinations of key geometric design elements and other critical elements were evaluated to assess their impact on vehicle stability when encountering a range of frictions between the traveled way and shoulder. These include vehicle type, vehicle speed, vehicle path, slope ratio, roadway curvature, and friction of slope ratio. The stability of the vehicle will be measured by the vehicle's roll angle. A rollover is defined as any vehicle rotation of 90 degrees or more about any true longitudinal or lateral axis, according to NASS CDS. For this study, a fixed superelevation was assumed. After all vehicle rollover scenarios were created and data was collected, LS-OPT was used to create metamodels.

Vehicle Dynamics Simulations

To run simulations on CarSim, several parameters must be specified. Figure 1 shows a flowchart on how simulations are created. Figure 2 is an image of the CarSim run control screen. From this screen, the vehicle used, the procedure, and the road must be specified. First, the vehicle is chosen. In this study, a Class C Hatchback vehicle and a Full-size SUV will be utilized. Figures 4 and 5 show images of the two vehicles used. The Class C Hatchback had a 1270 kg rigid sprung mass and the Full-size SUV had a 2257 kg rigid sprung mass. These masses are preset in CarSim and were not changed. The SUV had an ABS breaking system. Next, the procedure must be defined. Figure 3 shows an image of the graphic user interface on the procedure screen. The driving maneuver was specified in the procedures in CarSim. Plot definitions, driver controls, start, and stop conditions were also defined in the procedures. For this study, the vehicle has a set initial speed, no braking, and no steering. 8 different speeds were

also utilized. The encroachment angle is specified in the miscellaneous data field. The start and stop time of the runs is also specified here. Roads with varying slope ratio, and frictions were built in CarSim in order to run simulations. Slope ratio ranged from 3:1 to 4:1. The friction of the slope ratio ranged from 0.8 to 1.5. The roads used also had two curvatures; a road with a 621.79-meter radius and a road with an infinite radius. These were achieved utilizing the Road segment builder in CarSim. Table 6 shows the variation in design variables utilized in the study. Figures 10 and 11 show the two roads used in this study. Figures 12 and 13 depict a profile of the roads. The side-slopes were intentionally created to be very long in order to be able to see how the side-slope affected the roll angle and not the ditch. All these parameters (vehicle, procedure, and roadway) are specified in the Run Control Screen pictured in Figure 2. After all parameters were specified, the math model was run. Plots were then analyzed and data was gathered to be input into LS-OPT.

Metamodeling

LS-OPT allows the user to structure the design process, explore the design space, and compute optimal designs according to specified constraints and objectives. A total of 282 rollover scenarios were created using CarSim. These were divided into different datasheets by vehicle type, road curvature, encroachment angle, and side-slope ratio. To use LS-OPT, the metamodel type must first be chosen. LS-OPT offers 7 types of metamodels; polynomial, sensitivity, feedforward neural network, radial basis function network, kriging, support vector regression, and user defined. After several attempts, Feedforward Neural Network was chosen as the best metamodel for this study. Global sensitivities were also calculated. After the metamodel

type was chosen and the data was imported, the model was run. Figure 10 shows a picture of the LS-OPT user interface.

RESULTS

Vehicle Dynamics Simulation Results

A total of 282 rollover scenarios were created on CarSim. Of these runs, 34% (95 scenarios) resulted in vehicle rollover. A rollover is defined as any vehicle rotation of 90 degrees or more about any true longitudinal or lateral axis, according to NASS CDS. For this study, vehicles having a roll angle of 65 degrees or greater were labeled as being rolled over. Of those 95 rollovers, 57 were SUV rollovers and 38 were Class C Hatchbacks. More vehicles rolled over on the curved road than on the straight road. Also, vehicles were more likely to rollover on the 3:1 slope than on the 4:1 slope.

Metamodeling Results

The raw data from CarSim were separated into datasheets to be input into LS-OPT. Each data sheet had a varying vehicle type, a side-slope ratio, roadway curvature, and encroachment angle. Figure 11 is a flowchart of how the LS-OPT metamodels are categorized. The two metamodels discussed are the surface metamodel, and the Global Sensitivity Analysis. The two variables discussed will be the vehicles' roll angle and the maximum deviation from the centerline of the right lane. The results of the analysis are shown as a response surface in figures 12 through 43. In all the graphs, roll angle is in degrees, maximum deviation is in meters (m), speed is in kilometers per hour (Km/h), and friction factor is dimensionless. All the graphs are a function of speed and friction.

Full Size SUV Metamodels

Figures 12 through figure 19 show the various metamodels of the roll angle for SUV's travelling on a curved or straight roads with a 3:1 or 4:1 side-slope at a 15 or degree encroachment angle. For all 8 cases, speed had a greater influence on roll angle than did the friction of the side-slope. The greatest influence that friction had on a scenario was 14%. Rollover scenarios on the curved road tend to rollover at a slower speed than those on a straight road. This statement also holds true for rollover scenarios with a 25 degree encroachment angle. SUV's would rollover at a lower speed if the side-slope had a greater friction value.

Figures 20 through 27 show metamodels of the maximum deviation for SUV's travelling on a curved or straight road with a 3:1 or 4:1 side-slope at a 15 or 25 degree encroachment angle. For all 8 scenarios, speed had a greater influence on the vehicle's roll angle. The highest influence that friction experienced was 34%. For a majority of the scenarios, the metamodels surface is linear. 3 of the figures experience a spike in the surface at a low friction and high speed.

Class C Hatchback Metamodels

Figures 28 through figure 35 show the metamodels of the roll angle for Class C hatchbacks travelling on a curved or straight road with a 3:1 or 4:1 side-slope at a 15 or 25 degree encroachment angle. Similar to the SUV metamodels, the cars travelling on a curved road rolled over at a slower speed than those travelling on a straight road. The cars also had a higher propensity to roll over at a higher encroachment angle.

Figures 36 through 43 show metamodels of the maximum deviation for car's travelling on a curved or straight road with a 3:1 or 4:1 side-slope at a 15 or 25 degree encroachment angle. For all 8 scenarios, speed had a greater influence on the vehicle's roll angle. The highest influence

that friction experienced was 16%. For a majority of the scenarios, the metamodels surface is linear. 1 of the figures experienced a spike in the surface at a low friction and high speed.

DISCUSSION

The most prominent surface for the roll angle created on LS-OPT was one similar to Figure 33. For this surface at a speed less than 100 km/hr., vehicles experienced a higher roll angle on a higher friction surface. Metamodels for the SUV's had a steeper transition into the higher roll angle than the metamodels for the car. This indicates that SUV's are more likely to roll over than the class C hatchback. This may be due to the static stability factor mentioned in the background information under the fundamentals of vehicle dynamics section. The height of the center of gravity for an SUV is usually higher than that of a car. A higher CG height yields a smaller static stability factor. The lower the stability factor, the more likely the vehicle is to rollover. Vehicles with a 15-degree encroachment angle were less likely to roll than those traveling at a 25-degree angle. Most vehicles departing the road at a 25-degree angle were able to navigate back onto the road successfully. The vehicles were also more likely to roll over on a 3:1 slope than on the 4:1 slope. This is due to the steeper slope of the 3:1 slope compared to the 4:1 slope. It is important to study factors of roadway design since these are factors that can be changed to create safer roadway conditions. The maximum deviation from the centerline of the right lane was influenced more by the speed than by the friction of the road. The highest influence that friction experience was 34% for the SUVs. The surface metamodels were mainly linear. As the speed of the vehicle increased, the vehicles deviated further from the road. The friction of the road was held constant and the friction for the side-slope varied from 0.8 to 1.5. For most cases, as the friction increased the vehicle's propensity to rollover increased as well. This may be from the increase in the resisting forces acting on the tires. Wet road conditions

have been studied to better understand and help prevent events such as hydroplaning. Wet roads make roads less safe to drive on especially at lower temperatures when roads may freeze over. NCHRP Project 17-22 on the Identification of vehicular impact conditions associated with serious ran-off road crashes was conducted to identify vehicle types, impact conditions, and site characteristics associated with serious injury and fatal crashes involving roadside features and safety devices [14]. Police reported crashes are the most common type of crash data available. Police officers are required by law to investigate all reportable crashes and complete police accident reports. These reports are usually limited in detail. It was concluded that utilizing enhanced police level crash reports using investigating officers to collect supplemental data could provide more detailed information on the impact conditions of single vehicle, ran-off road crashes. To properly estimate the impact conditions of single-vehicle, ran-off road crashes, an in depth level of crash investigation is required. Required data would include vehicle trajectory, objects struck, vehicle and damage measurements, and driver and occupant injury levels. The Federal Highway Administration's Rollover study [15] and NCHRP Project 17-11 incorporated the same data collection procedures used in NCHRP 17-22. Data from NCHRP 17-11 showed that 50% of vehicles rolled over [14]. NCHRP 17-22 showed a 50% rollover rates for cars and 69% for light trucks. These numbers are similar to the current study in that the Full-Size SUV was more likely to rollover than the Class C Hatchback. One cannot control how drivers navigate the road but posted speeds, and other roadway characteristics such as side-slope and ditches are factors that can be modified for safer roads. There is no set roll angle at which all cars will rollover since there are many factors that influence the vehicle's propensity to rollover. It can be inferred that as a vehicle's roll angle increases, the vehicle's ability to navigate a road safely decreases.

CONCLUSIONS

The main goal of this research was to enhance our understanding of a vehicles' propensity to rollover using vehicle dynamics simulations instead of crash data. The rollover crash is one of the most fatal forms of crashes among passenger vehicles. In 2015, they accounted for one third of all occupant fatalities. 48% of crashes occurred in rural roads and 45% occurred in urban roads. The percentage of fatalities in rollover crashes was highest for SUVs, followed by pickup trucks, vans, and passenger cars. Utilizing CarSim and LS-OPT, vehicle rollover scenarios and metamodels were built. For vehicle simulations, a fixed superelevation of 6% was assumed. Two road curvatures, two side-slopes, 7 different speeds and 2 encroachment angles were used to create the simulations. A total of 282 rollover scenarios were created on CarSim. It was deduced that:

- Side-slopes and ditches have been identified as the primary tripping mechanisms in single vehicle ran-off road rollovers.
- Full Size SUV was more likely to rollover than the Class C Hatchback due to its static stability factor. This is similar to data from NCHRP 17-22 showing that light trucks are more likely to rollover than cars.
- Speed has a greater influence on the vehicle's propensity to rollover.
- Friction held a greater influence on the vehicle's deviation from the centerline of the right lane.
- The vehicle's travelling at a 25 degree encroachment angle are more likely to roll over than those travelling at a 15 degree angle.

It is important to study factors of roadway design since these are factors that can be changed to create safer roadway conditions. One cannot control how drivers navigate the road but posted speeds, and other roadway characteristics such as side-slope and ditches are factors that can be modified for safer roads. For future work, more variables are to be studied and implemented to utilize data analytics. Data analytics has shown great promise and usefulness in many sciences and industries where large amount of data (Big Data) has to be analyzed for trends, sensitivities and probabilistic prediction of desired responses. Advanced algorithms, approaches and tools have been developed in response to the exponential growth of data in many fields including transportation. Researchers recommend using a data analytics utility to address the desired vehicular responses as functions of roadway and roadside variables. The approach recommended is to construct extensive database of the desired responses, design variables and encroachment conditions via massive simulation runs. Then, a higher order meta-model (response surface) is to be constructed. Subsequently, this constructed meta-model can be used for probabilistic analyses to develop sensitivities, trends and probabilities via Monte Carlo simulation. Ditches, roadway shoulders, and tire-soil interaction are a just a few that can be implemented.

REFERENCES

- [1]. National Highway Traffic Safety Administration. “Rural/Urban Comparison of Traffic Fatalities.” April 2017.
<https://crashstats.nhtsa.dot.gov/Api/Public/ViewPublication/812393>. Accessed Jul. 31, 2017.
- [2]. Kahane, C.J. 2012. “Relationships between fatality risk, mass, and footprint in model year 2000-2007 passenger cars and LTVs — final report.” Report no. DOT HS-811-665. Washington, DC: National Highway Traffic Safety Administration.
- [3]. Deutermann, W. 2002. “Characteristics of fatal rollover crashes.” Report no. DOT HS-809-438. Washington, DC: National Highway Traffic Safety Administration.
- [4]. American Association of State Highway and Transportation Officials. *Roadside Design Guide*. Washington, DC. 2011.
- [5]. American Association of State Highway and Transportation Officials. *A Policy on Geometric Design of Highways and Streets*. Washington, DC. 2011.
- [6]. Viner, J. G. 1995. “Rollovers on Sideslopes and Ditches,” *Accident Analysis & Prevention* 27(4): 483–491.
- [7]. Gillespie, T. D. *Fundamentals of Vehicle Dynamics*. Thomas D. Gillespie. Warrendale, PA : Society of Automotive Engineers, [1992], 1992.
- [8]. Huston, R.L. and F.A. Kelly. “Another Look at the Static Stability Factor (SSF) in Predicting Vehicle Rollover.” *International Journal of Crashworthiness*, vol. 19, no. 6, 01 Nov. 2014, p. 567-575. EBSCOhost, doi:10.1080/13588265.2014.919730.

- [9]. Aarts, L., and van Schagen, I., “Driving speed and the risk of road crashes: A review.” *Accident analysis and prevention* 38.2 (2006):215-224. Web.
- [10]. Kim, J.-H., S. Hayakawa, T. Suzuki, K. Hayashi, S. Okuma, N. Tsuchida. “Modeling of Driver's Collision Avoidance Maneuver Base on Controller Switching Model.” *IEEE Transactions on Systems, Man, and Cybernetics, Part B: Cybernetics*, 35 (6), 1131-1143. IEEE Systems, Man, and Cybernetics Society. New York, NY. 2005.
- [11]. Allen, R. and Rosenthal, T., “Requirements for Vehicle Dynamics Simulation Models,” SAE Technical Paper 940175, 1994, <https://doi.org/10.4271/940175>.
- [12]. LS-OPT User’s Manual Version 5.2, Livermore Software Technology Corporation, Livermore, 2015.
- [13]. Karayiannis N.B., Venetsanopoulos A.N. (1993) Neural Network Architectures and Learning Schemes. In: Artificial Neural Networks. The Springer International Series in Engineering and Computer Science, vol 209. Springer, Boston, MA
- [14]. NCHRP Project 17-11, “Recovery-Area Distance Relationships for Highway Roadsides,” ongoing study conducted by Texas Transportation Institute, Texas A&M University System, College Station, Texas.
- [15]. Mak, K. K., and D. L. Sicking, “Rollover Caused by Concrete Safety Shaped Barrier,” Final report, prepared for Federal Highway Administration, U. S. Department of Transportation, Washington, D. C., September 1988.

Supplemental Sources Consulted

Alvarez, A., et al. “Vehicle Dynamics Simulation at Commercial Vehicle Development.” SAE technical paper series Vehicle Dynamics Simulation at Commercial Vehicle Development. 1. Web.

Farmer, Charles M, Richard A Retting, and Adrian K Lund. "Changes in motor vehicle occupant fatalities after repeal of the national maximum speed limit." *Accident analysis and prevention* 31.5 (1999):537-543. Web.

Garcia, R., October 2014, *Roadway Design Manual*.

<http://onlinemanuals.txdot.gov/txdotmanuals/rdw/rdw.pdf>. Accessed July 31, 2017.

Kimley-Horn and Associates, May 2013, "Traffic Safety Evaluation for SR 147 MP 7 to MP 14." <http://www.zerofatalitiesnv.com/wp-content/uploads/2015/10/SR-147-Lake-Mead-Report.pdf>. Accessed July 31, 2017.

Lave, Charles, and Patrick Elias. "Did the 65 mph speed limit save lives?." *Accident analysis and prevention* 26.1 (1994):49-62. Web.

Renski, Henry, Asad Khattak, and Forrest Council. "Effect of Speed Limit Increases on Crash Injury Severity: Analysis of Single-Vehicle Crashes on North Carolina Interstate Highways." *Transportation research record* 1665(1999):100-108. Web.

Rice, R.S. and F. Dell'Amico. "An Experimental Study of Automobile Driver Characteristics and Capabilities." *Calspan Report No. ZS-5208-K-1*. Calspan Corporation. Buffalo, NY. March 1974.

Whitehead, R., et al. "A Study of the Effect of Various Vehicle Properties on Rollover Propensity." *SAE Conference Proceedings P*, vol. 386, 2004, pp. 205-212.

Zhen-Feng Wang. et al. "Influence of Road Excitation and Steering Wheel Input on Vehicle System Dynamic Responses." *Applied Sciences (2076-3417)*, vol. 7, no. 6, June 2017, pp. 1-23.

Maeda, T., N. Irie, K. Hidaka, and H. Nishimura. "Performance of Driver-Vehicle System in Emergency Avoidance." International Automotive Engineering Congress and Exposition. Society of Automotive Engineers. Detroit, MI. 1977.

CarSim, Mechanical Simulation Corporation, <http://www.carsim.com>.

Viano, D. C., and Parenteau, C., *Occupant and Vehicle Responses in Rollovers*. Warrendale, PA, Society of Automotive Engineers, 2004.

APPENDIX A

TABLES

Table 1. Texas Fatalities by crash type

Crash Type	2012	2013	2014	2015	2016
Total Fatalities (All Crashes)*	3,408	3,389	3,536	3,582	3,776
Single Vehicle	55%	54%	54%	52%	52%
Involving a Large Truck	17%	16%	16%	16%	15%
Involving Speeding	37%	35%	36%	31%	28%
Involving a Rollover	30%	30%	31%	27%	27%
Involving a Roadway Departure	53%	54%	54%	50%	49%
Involving an Intersection (or Intersection Related)	19%	20%	19%	20%	19%

Table 2. Passenger vehicle occupant deaths in single-vehicle rollover crashes, 1978-2015

Year	Car drivers	Pickup drivers	SUV drivers	All passenger vehicle drivers	All passenger vehicle occupants
1978	3,710	1,140	271	5,323	7,858
1979	3,610	1,263	329	5,396	8,010
1980	3,995	1,309	406	5,895	8,673
1981	3,826	1,291	364	5,687	8,211
1982	3,222	1,162	312	4,828	6,974
1983	3,169	1,120	319	4,732	6,951
1984	3,252	1,226	331	4,964	7,116
1985	3,076	1,202	360	4,773	6,900
1986	3,474	1,401	375	5,400	7,954
1987	3,427	1,535	403	5,528	8,162
1988	3,675	1,656	447	5,925	8,562
1989	3,309	1,629	463	5,551	8,060
1990	3,291	1,563	486	5,477	8,068
1991	3,092	1,595	470	5,282	7,749

1992	2,800	1,492	442	4,848	7,135
1993	2,664	1,462	494	4,729	7,002
1994	2,826	1,403	522	4,879	7,268
1995	3,005	1,556	602	5,284	7,802
1996	2,932	1,514	720	5,294	7,903
1997	2,818	1,469	754	5,178	7,712
1998	2,857	1,545	808	5,328	7,848
1999	2,866	1,667	999	5,644	8,255
2000	2,795	1,526	1,035	5,466	8,112
2001	2,836	1,651	1,063	5,654	8,375
2002	2,977	1,668	1,224	5,967	8,724
2003	2,755	1,595	1,331	5,789	8,462
2004	2,706	1,540	1,490	5,853	8,525
2005	2,761	1,711	1,478	6,074	8,730
2006	2,764	1,754	1,555	6,198	8,790
2007	2,634	1,683	1,516	5,934	8,429
2008	2,354	1,537	1,398	5,380	7,541
2009	2,101	1,478	1,273	4,913	6,868
2010	1,946	1,324	1,226	4,548	6,375
2011	1,848	1,297	1,218	4,430	6,148
2012	1,951	1,288	1,287	4,567	6,273
2013	1,805	1,219	1,112	4,181	5,825
2014	1,673	1,195	1,185	4,100	5,570
2015	1,775	1,202	1,205	4,243	5,766

Table 3. Deaths in single-vehicle crashed as a percent of all occupant deaths, 2015

		Drivers				All occupants			
		Single-vehicle rollover		All crashes		Single-vehicle rollover		All crashes	
		Number	%	Number	%	Number	%	Number	%
Cars	Mini	82	15	552	100	102	14	712	100
	Small	538	18	2,985	100	709	17	4,066	100
	Midsize	663	19	3,408	100	928	20	4,726	100
	Large	369	20	1,864	100	497	20	2,542	100
	Very large	100	16	626	100	146	15	989	100
	All cars	1,775	19	9,531	100	2,414	18	13,157	100
Pickups	Small	304	29	1,043	100	364	29	1,240	100
	Large	599	34	1,787	100	775	34	2,308	100
	Very large	253	44	569	100	330	44	748	100

	All pickups	1,202	34	3,523	100	1,532	34	4,467	100
SUVs	Small	246	29	855	100	322	29	1,122	100
	Midsize	648	40	1,633	100	934	40	2,354	100
	Large	226	45	504	100	340	44	766	100
	Very large	72	42	170	100	112	42	264	100
	All SUVs	1,205	38	3,192	100	1,724	38	4,545	100
All passenger vehicles	All	4,243	26	16,484	100	5,766	26	22,543	100

Table 4. Passenger vehicle occupant deaths in rollover vs. no rollover crashes, 1978-2015

Year	Car occupants				Pickup occupants				SUV occupants			
	Rollover		No rollover		Rollover		No rollover		Rollover		No rollover	
	Number	%	Number	%	Number	%	Number	%	Number	%	Number	%
1978	6,422	23	21,476	77	1,989	39	3,114	61	520	61	332	39
1979	6,416	23	21,102	77	2,222	41	3,201	59	630	67	315	33
1980	6,862	25	20,420	75	2,263	41	3,226	59	735	65	389	35
1981	6,541	25	19,865	75	2,177	42	3,059	58	663	65	358	35
1982	5,477	24	17,667	76	1,935	40	2,844	60	571	66	291	34
1983	5,381	24	17,420	76	1,939	42	2,721	58	609	66	311	34
1984	5,525	24	17,957	76	2,048	42	2,836	58	587	66	299	34
1985	5,219	23	17,857	77	2,044	42	2,848	58	671	66	353	34
1986	5,996	24	18,884	76	2,371	44	2,963	56	737	65	394	35
1987	5,997	24	19,118	76	2,598	45	3,197	55	824	65	445	35
1988	6,227	24	19,598	76	2,762	45	3,327	55	815	62	505	38
1989	5,784	23	19,485	77	2,680	45	3,336	55	847	62	526	38
1990	5,695	23	18,718	77	2,713	45	3,319	55	910	61	570	39
1991	5,443	24	17,295	76	2,593	44	3,265	56	934	61	587	39
1992	4,944	23	16,880	77	2,479	45	2,997	55	879	63	511	37
1993	4,865	22	17,252	78	2,415	43	3,196	57	971	63	581	37
1994	5,112	23	17,510	77	2,393	43	3,211	57	1,102	61	707	39
1995	5,340	23	17,784	77	2,581	43	3,392	57	1,257	63	749	37
1996	5,323	23	18,104	77	2,539	43	3,389	57	1,429	65	781	35
1997	5,143	22	18,019	78	2,479	42	3,443	58	1,516	63	900	37
1998	5,122	23	17,235	77	2,537	43	3,367	57	1,703	63	1,008	37
1999	5,174	23	16,945	77	2,699	44	3,396	56	1,901	63	1,118	37
2000	4,997	23	16,988	77	2,529	42	3,467	58	2,067	62	1,270	38
2001	5,028	23	16,576	77	2,636	43	3,485	57	2,159	61	1,362	39

2002	5,243	24	16,764	76	2,715	45	3,343	55	2,474	62	1,548	38
2003	4,916	23	16,137	77	2,509	43	3,324	57	2,658	60	1,805	40
2004	4,781	23	15,779	77	2,519	44	3,197	56	2,949	62	1,823	38
2005	4,830	24	15,062	76	2,773	46	3,267	54	2,909	60	1,938	40
2006	4,739	25	14,295	75	2,781	47	3,096	53	2,919	59	2,054	41
2007	4,400	25	13,363	75	2,660	46	3,098	54	2,929	59	2,046	41
2008	3,982	25	11,709	75	2,368	47	2,653	53	2,510	58	1,840	42
2009	3,509	25	10,593	75	2,246	48	2,473	52	2,388	56	1,866	44
2010	3,194	24	10,210	76	2,057	46	2,386	54	2,340	57	1,790	43
2011	3,058	24	9,653	76	1,973	46	2,272	54	2,259	55	1,836	45
2012	3,200	24	9,889	76	1,987	46	2,352	54	2,287	55	1,884	45
2013	2,984	23	9,720	77	1,916	45	2,299	55	2,057	50	2,041	50
2014	2,815	22	9,714	78	1,871	44	2,352	56	2,070	50	2,033	50
2015	2,965	23	10,192	77	1,909	43	2,558	57	2,203	48	2,342	52

Table 5. Center of gravity height, rollover threshold

Vehicle Type	CG Height (inches)	Tread (inches)	Rollover Threshold (G)
Sports car	18-20	50-60	1.2-1.7
Compact car	20-23	50-60	1.1-1.5
Luxury car	20-24	60-65	1.2-1.6
Pickup truck	30-35	65-70	0.9-1.1
Passenger van	30-40	65-70	0.8-1.1
Medium truck	45-55	65-75	0.6-0.8
Heavy truck	60-85	70-72	0.4-1.6

Table 6. Vehicle dynamics simulation matrix

Variables	Example Conditions
Ditch Geometry	3:1 and 4:1
Vehicle Speed (km/h)	65, 71, 80, 90, 110, 120, 130
Coefficient of Frictions for Tire-Terrain Friction (to represent soft soil conditions and various surface materials)	0.8, 0.9, 1.0 , 1.5

APPENDIX B

FIGURES

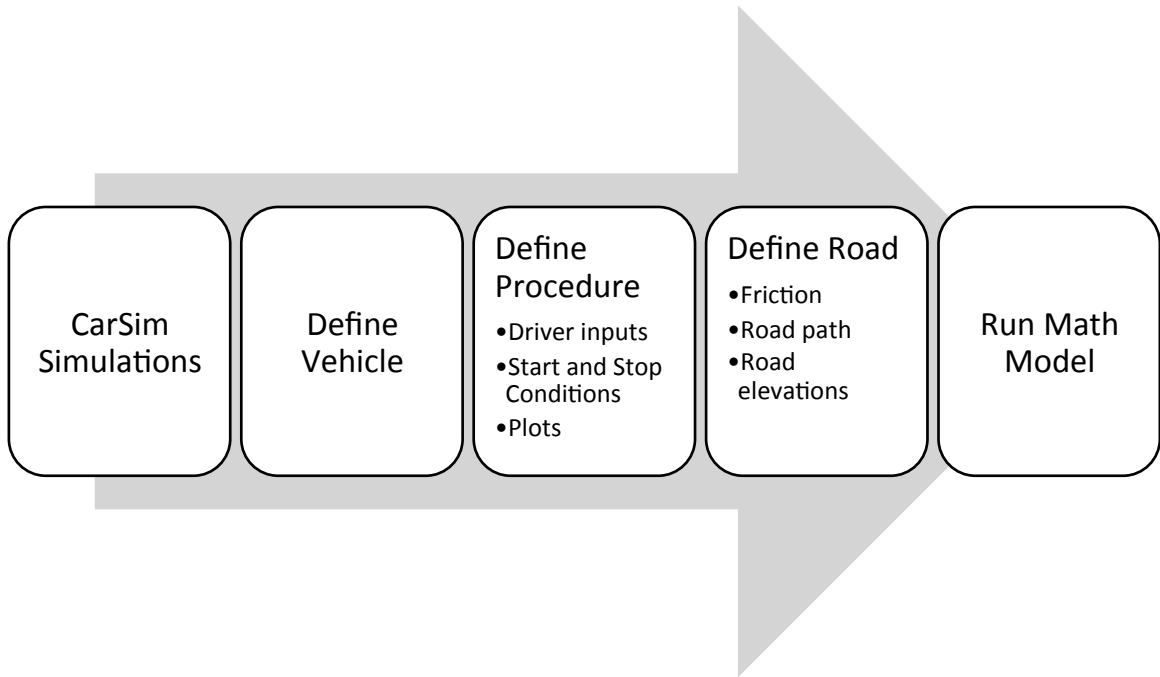


Figure 1. CarSim Simulation Flowchart

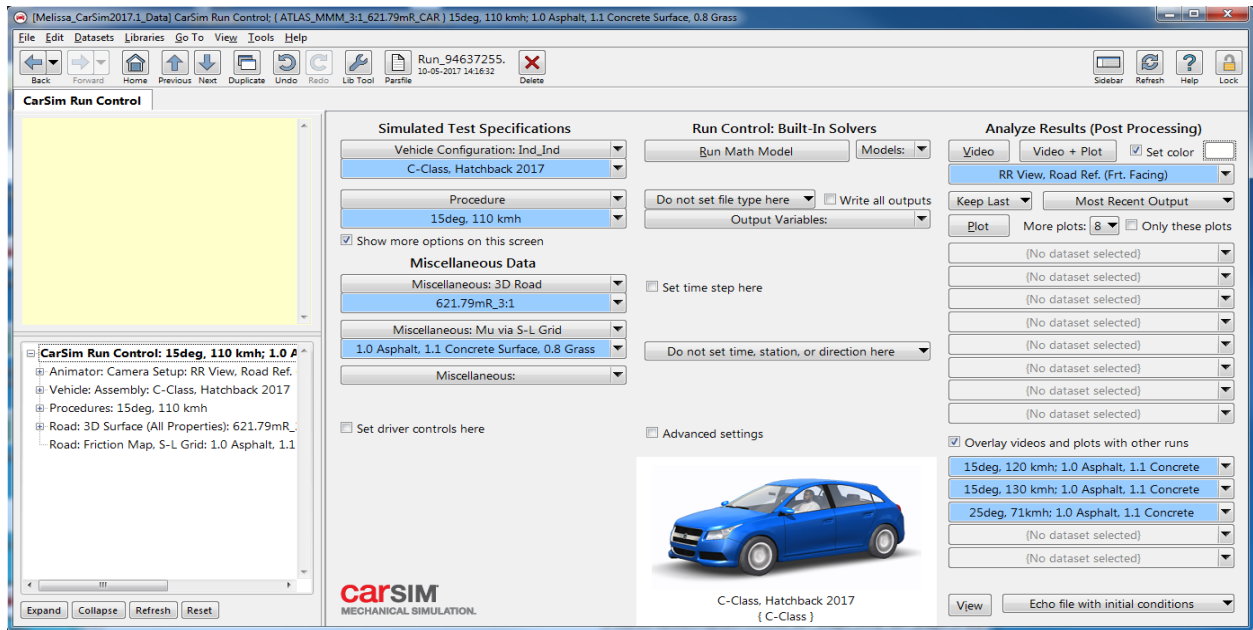


Figure 2. CarSim Run Control Screen

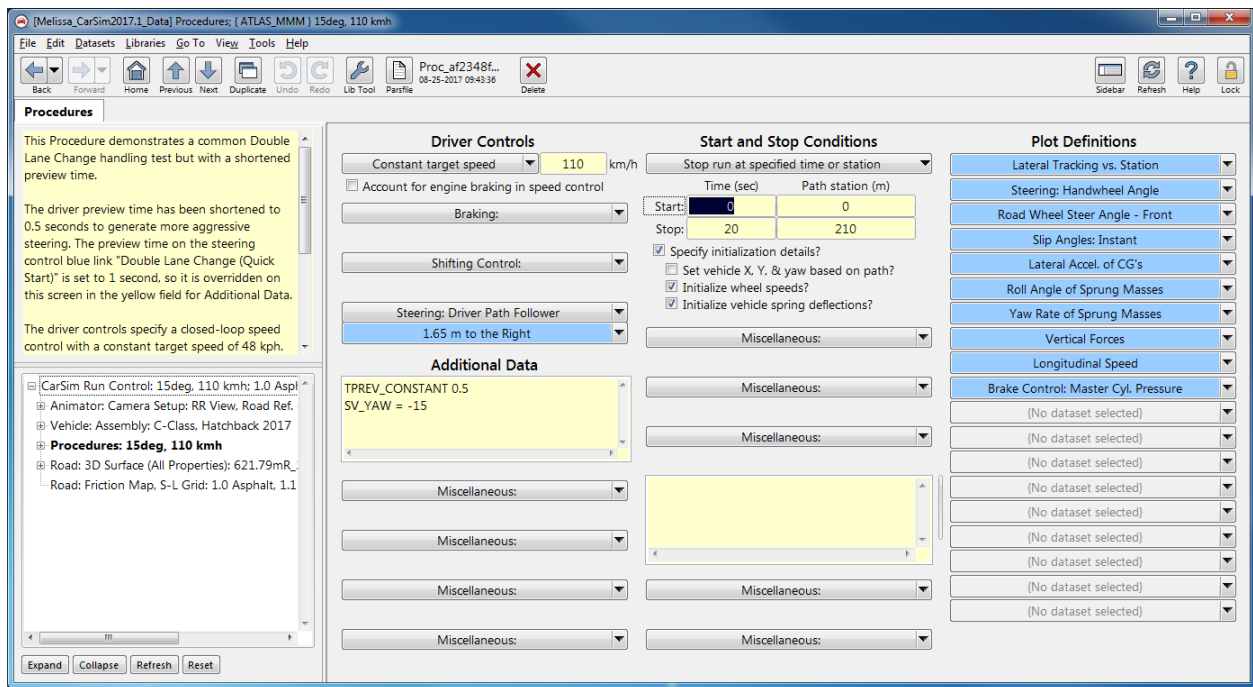


Figure 3 CarSim Procedures Screen



Figure 4 Class C Hatchback



Figure 5 Full-Size SUV



Figure 6 621.79 meter radius road with a 3:1 side-slope



Figure 7. Straight road with a 3:1 side-slope

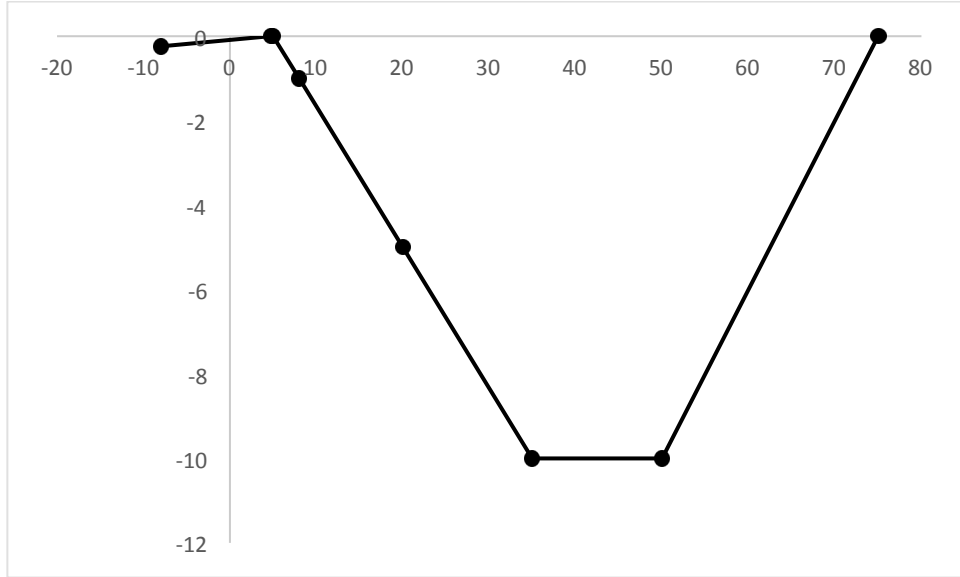


Figure 8. Road profile of the 3:1 side-slope

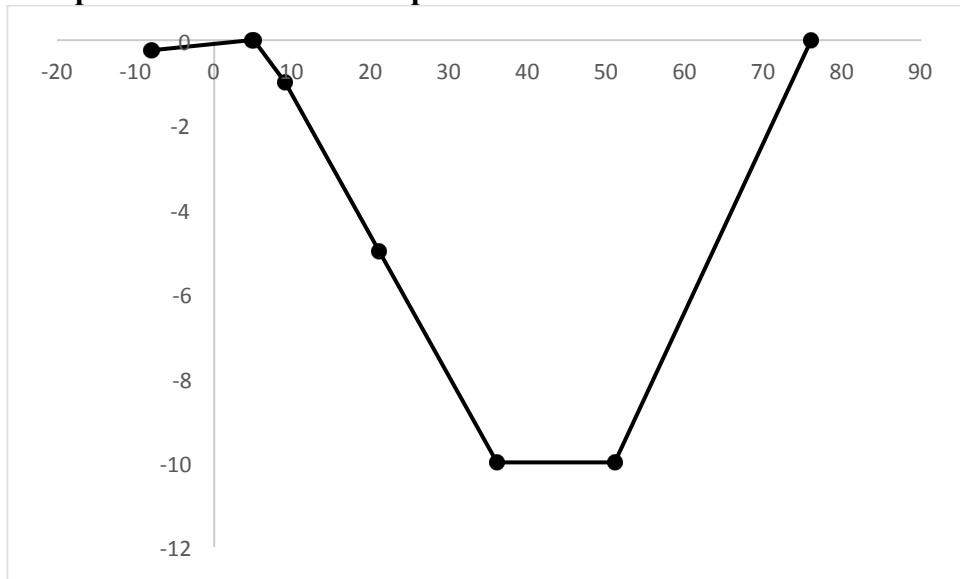


Figure 9. Road Profile of 4:1 side-slope

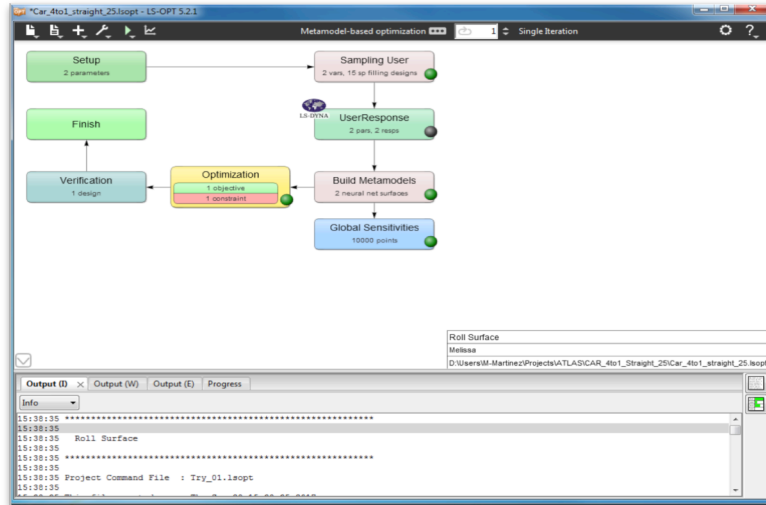


Figure 10. LS-OPT user interface

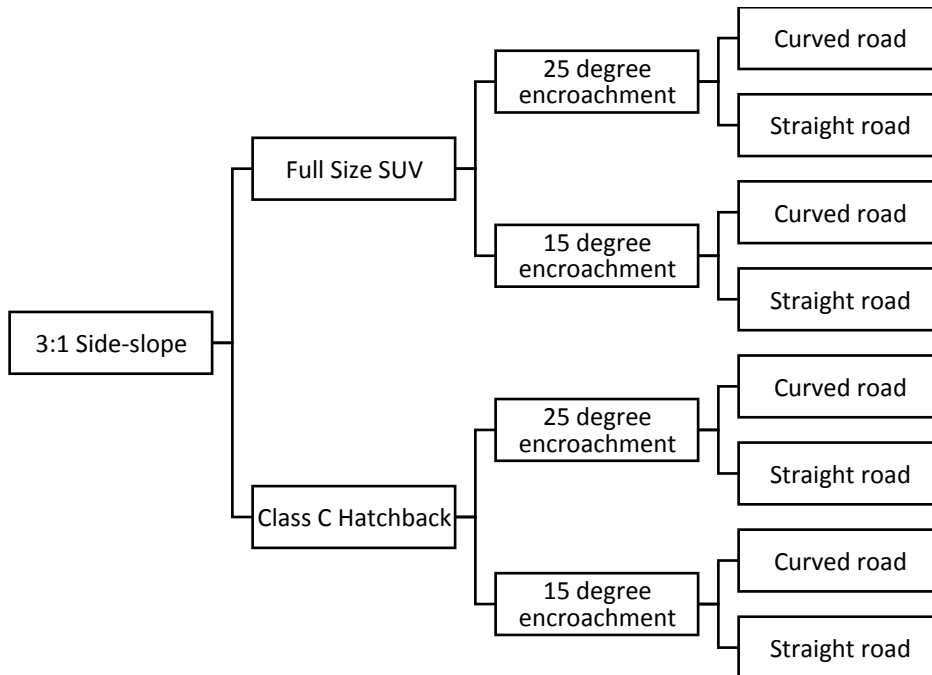
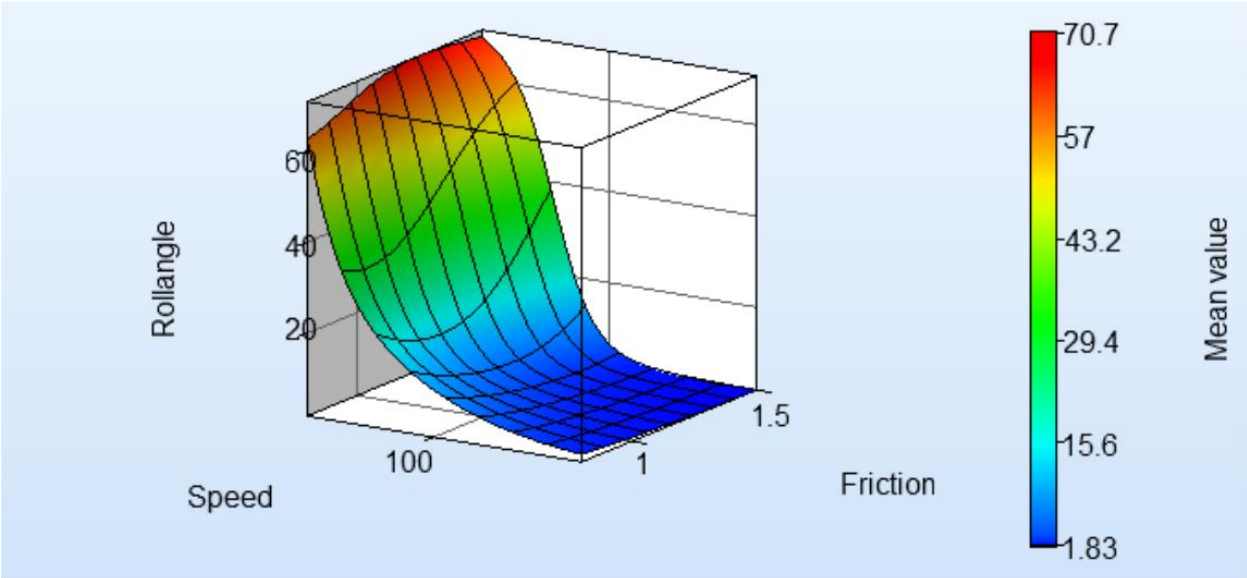


Figure 11 LS-OPT Categories



Global Sensitivities Plot for Rollangle
 Mean = 15.6458, Total variance = 348.476, Noise variance = 0.0212218

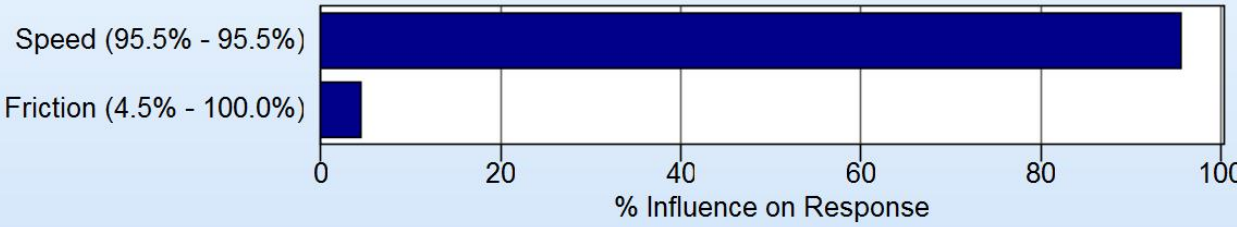
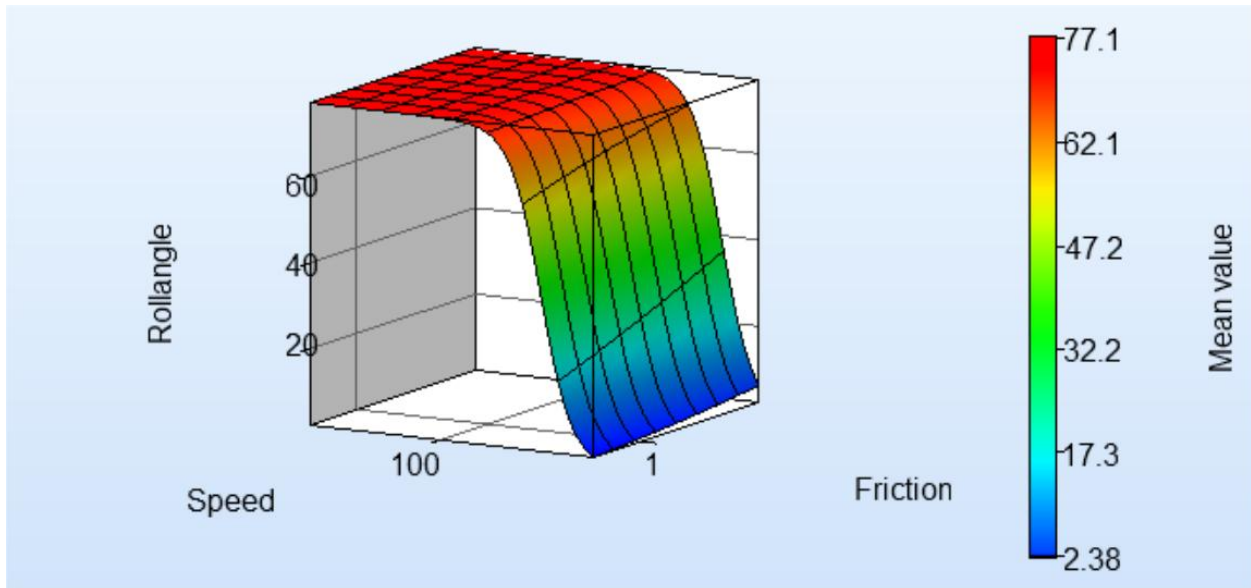


Figure 12. Surface Metamodel and Global sensitivity analysis: SUV, 3:1 curved road, 15 degree encroachment angle



Global Sensitivities Plot for Rollangle
 Mean = 64.769, Total variance = 485.394, Noise variance = 2.96896e-006

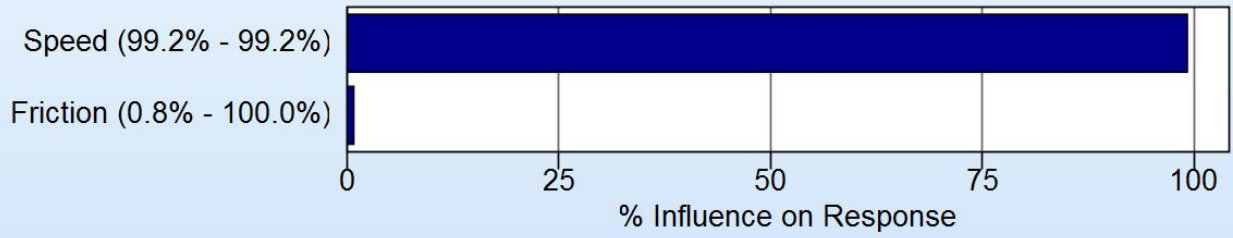
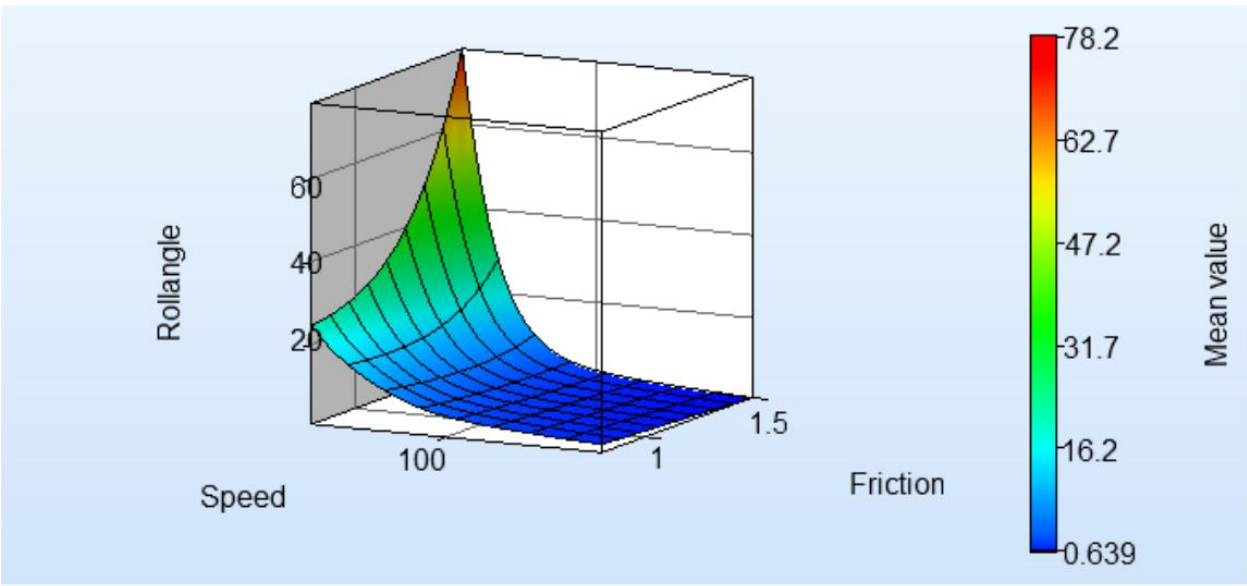


Figure 13. Surface Metamodel and Global sensitivity analysis: SUV, 3:1 curved road, 25 degree encroachment angle.



Global Sensitivities Plot for Rollangle
 Mean = 7.65892, Total variance = 76.0221, Noise variance = 1.42677

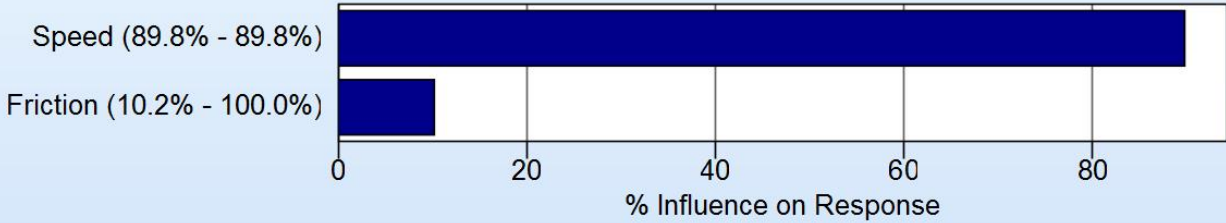
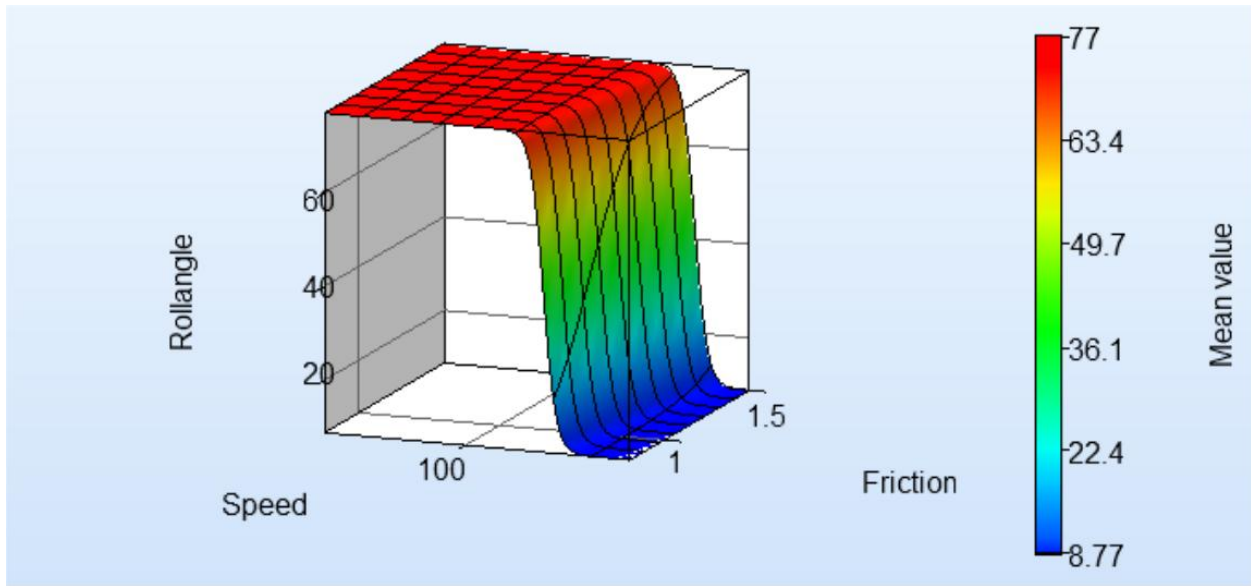


Figure 14. Surface Metamodel and Global sensitivity analysis: SUV, 3:1 straight, 15 degree encroachment angle



Global Sensitivities Plot for Rollangle
 Mean = 61.3045, Total variance = 729.029, Noise variance = 7.93493e-008

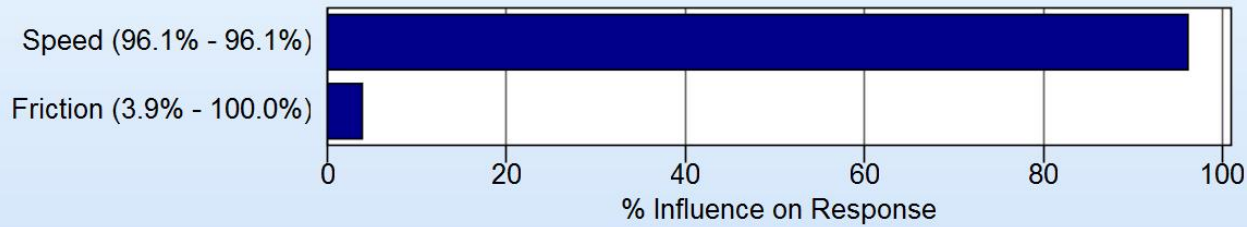
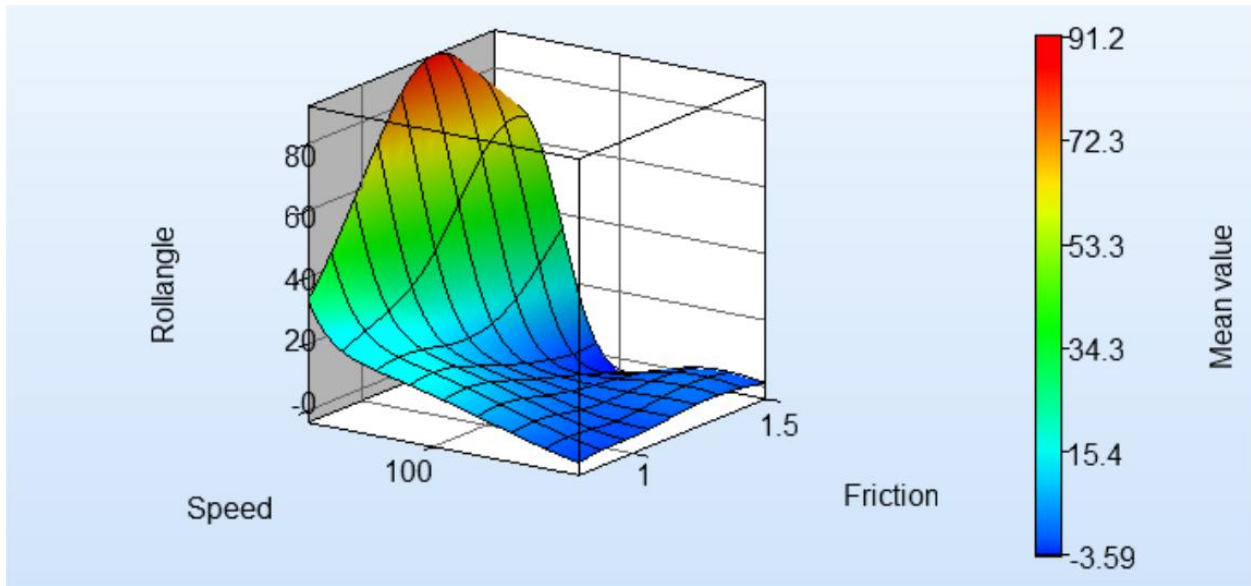


Figure 15. Surface Metamodel and Global sensitivity analysis: SUV, 3:1 straight road, 25 degree encroachment angle.



Global Sensitivities Plot for Rollangle
 Mean = 15.0832, Total variance = 403.893, Noise variance = 44.199

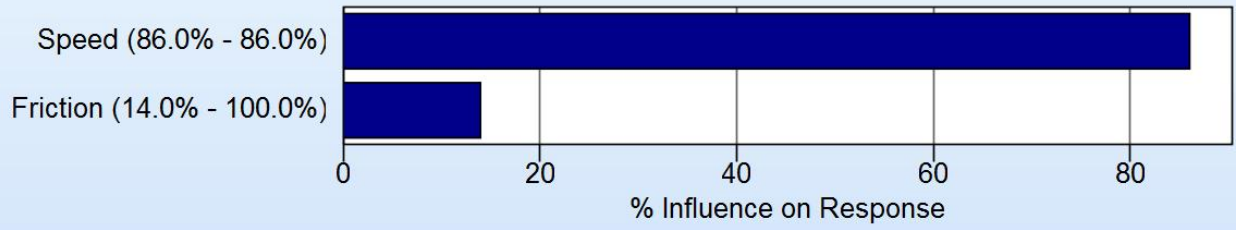
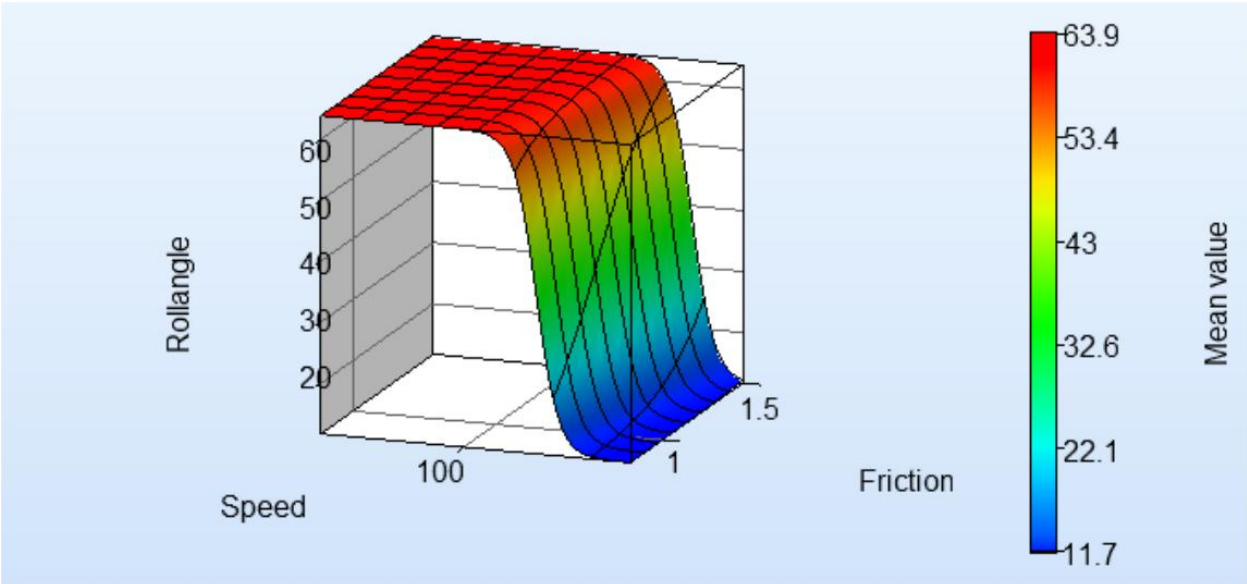


Figure 16. Surface Metamodel and Global sensitivity analysis: SUV, 4:1 curved, 15 degree encroachment angle.



Global Sensitivities Plot for Rollangle
 Mean = 51.7176, Total variance = 387.194, Noise variance = 1.19258e-005

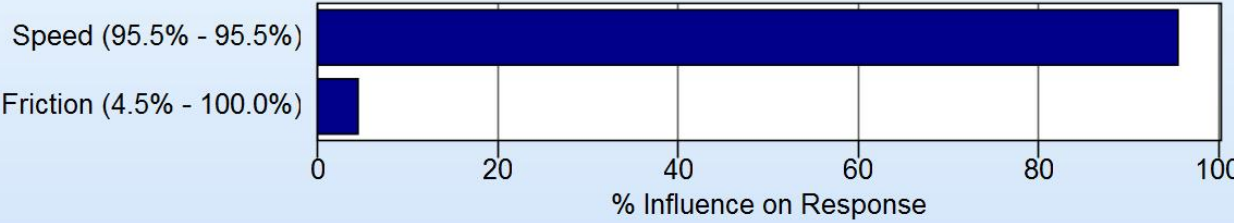
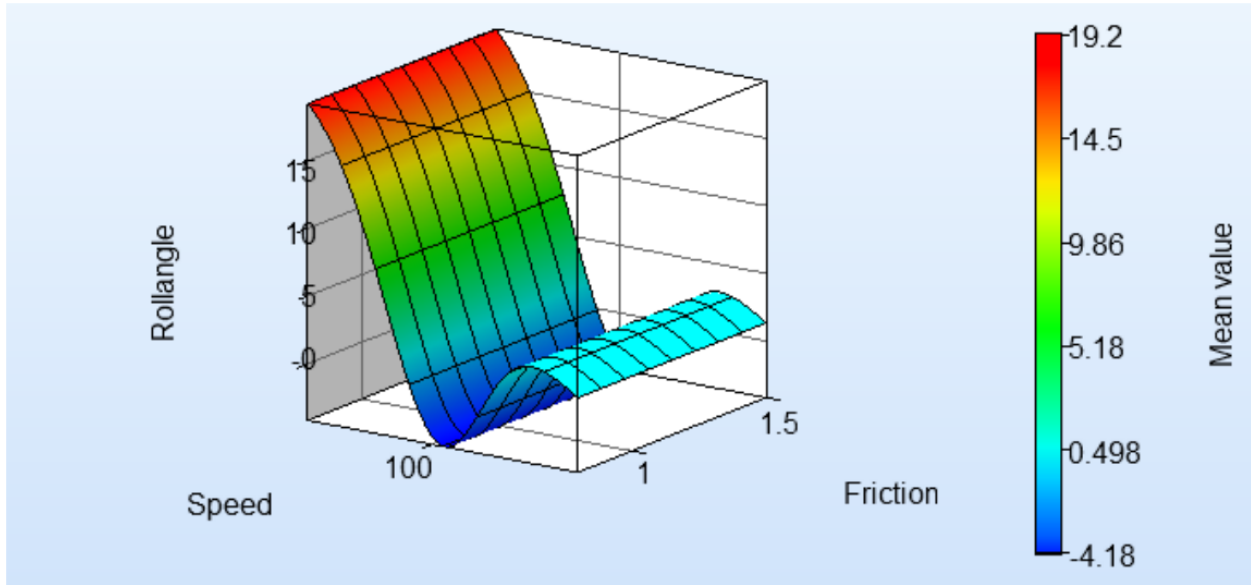


Figure 17. Surface Metamodel and Global sensitivity analysis: SUV, 4:1 curved road, 25 degree encroachment angle.



Global Sensitivities Plot for Rollangle
 Mean = 4.00354, Total variance = 45.6316, Noise variance = 11.5534

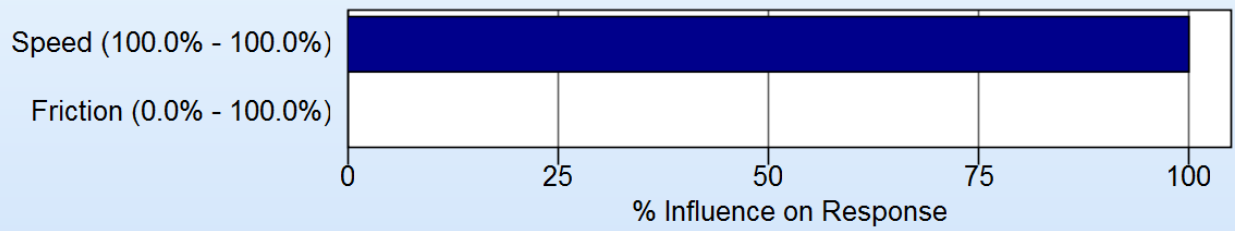
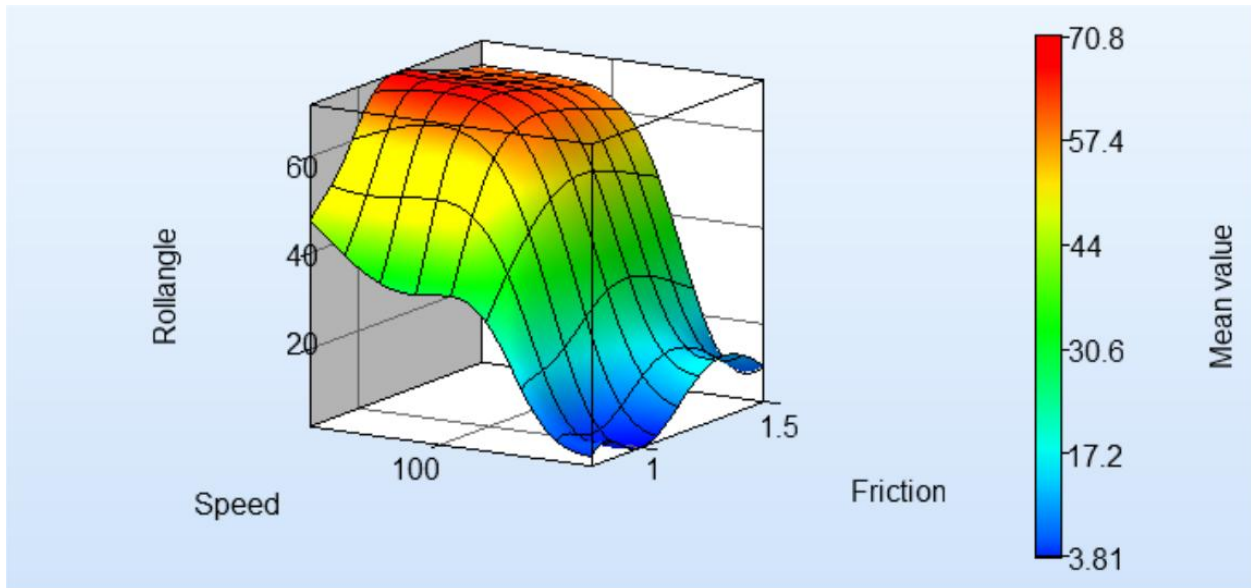


Figure 18. Surface Metamodel and Global sensitivity analysis: SUV, 4:1 straight road, 15 degree encroachment angle.



Global Sensitivities Plot for Rollangle
 Mean = 47.0713, Total variance = 478.545, Noise variance = 42.5656

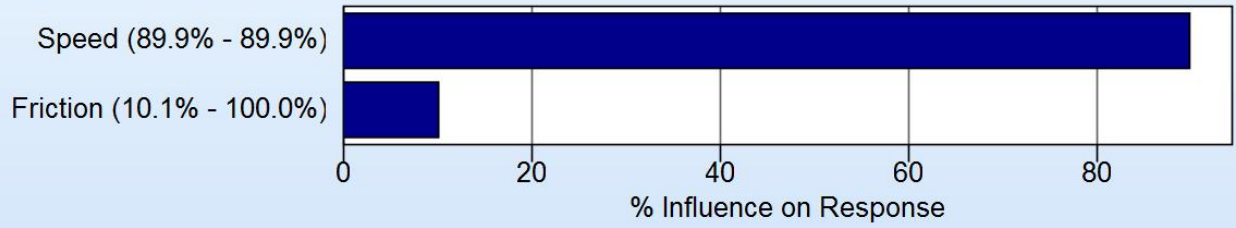
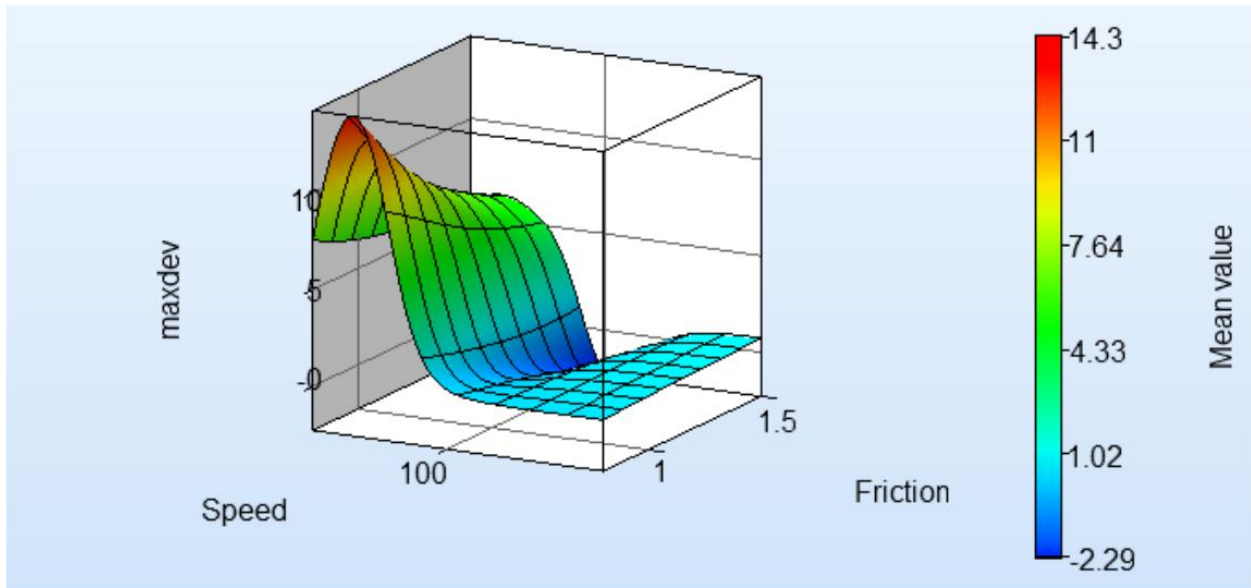


Figure 19. Surface Metamodel and Global sensitivity analysis: SUV, 4:1 straight road, 25 degree encroachment angle.



Global Sensitivities Plot for maxdev
 Mean = 2.72806, Total variance = 13.8477, Noise variance = 4.28984

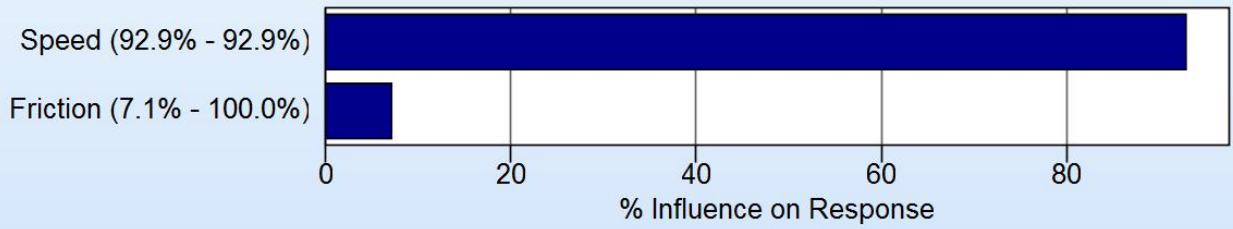
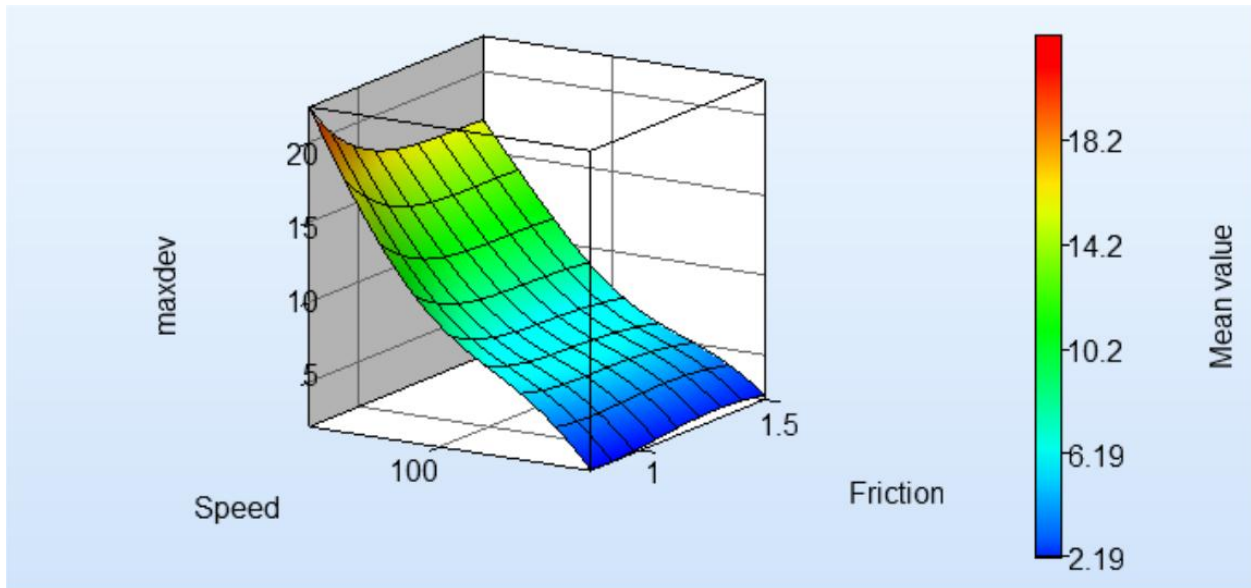


Figure 20. Surface Metamodel and Global sensitivity analysis: SUV, 3:1 curved road, 15 degree encroachment angle



Global Sensitivities Plot for maxdev
 Mean = 8.90582, Total variance = 17.3803, Noise variance = 0.106327

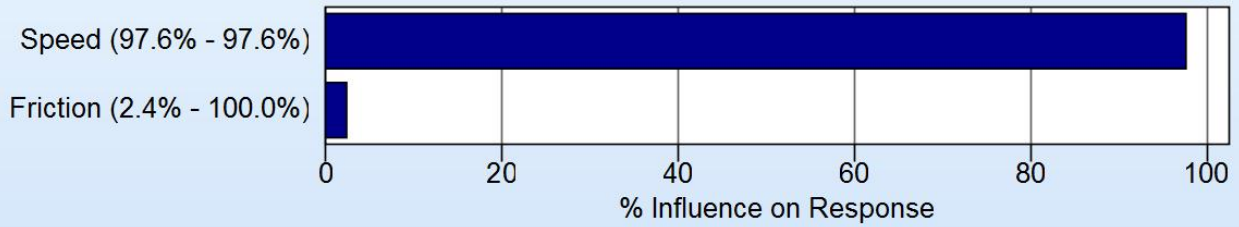
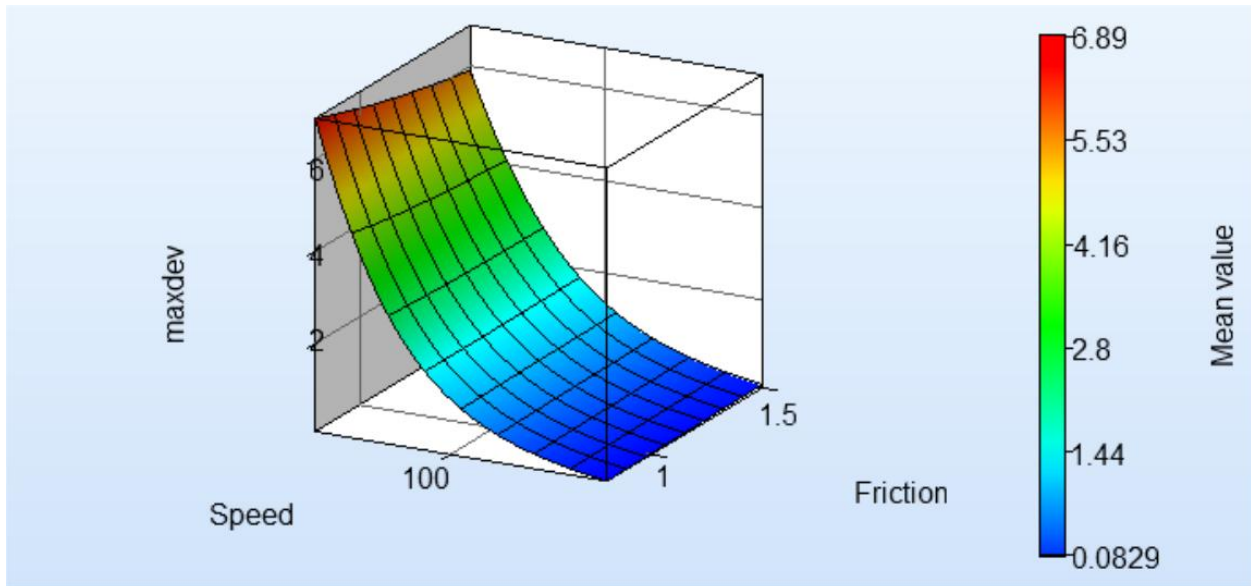


Figure 21. Surface Metamodel and Global sensitivity analysis: SUV, 3:1 curved road, 25 degree encroachment angle



Global Sensitivities Plot for maxdev
 Mean = 1.79168, Total variance = 2.80878, Noise variance = 0.0121671

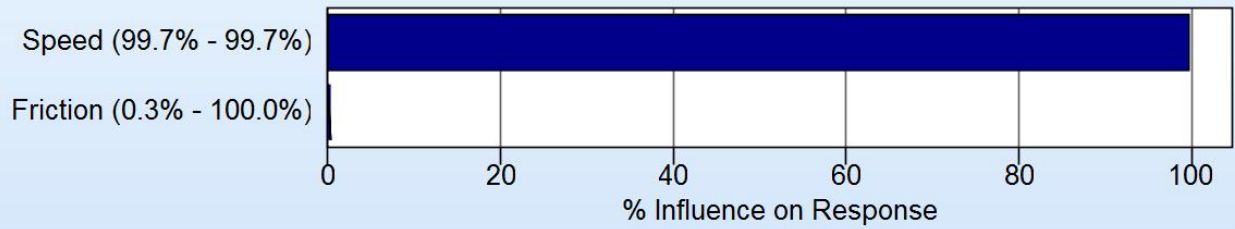
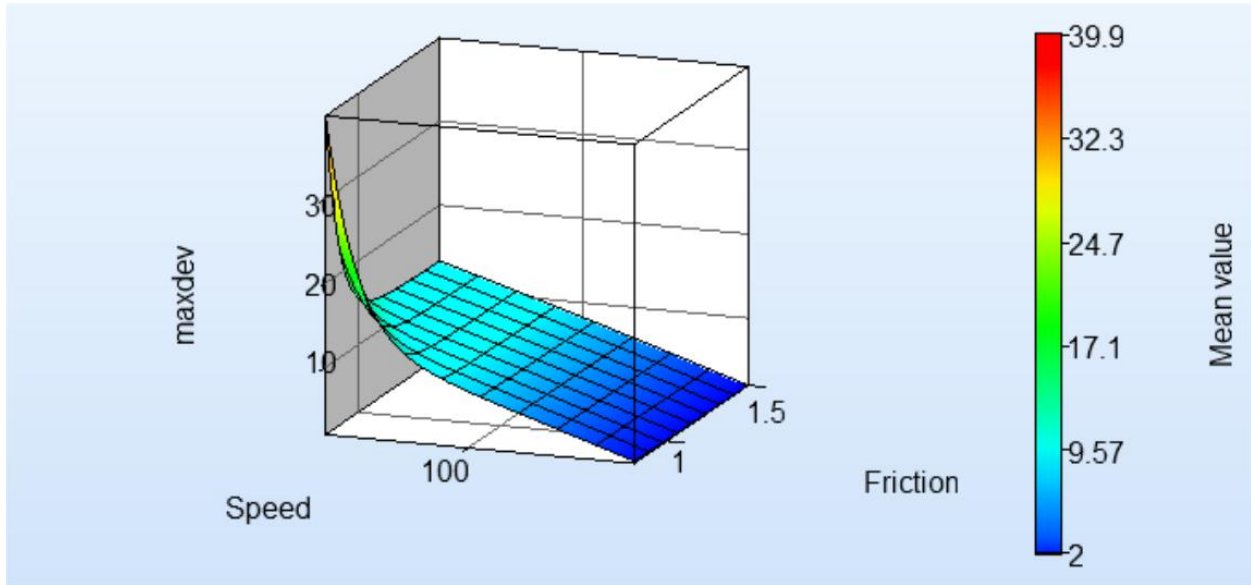


Figure 22. Surface Metamodel and Global sensitivity analysis: SUV, 3:1 straight road, 15 degree encroachment angle



Global Sensitivities Plot for maxdev
 Mean = 8.17249, Total variance = 15.0266, Noise variance = 0.00434049

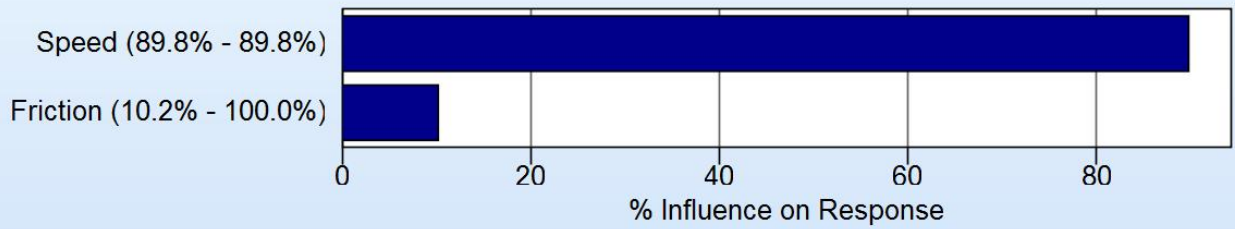
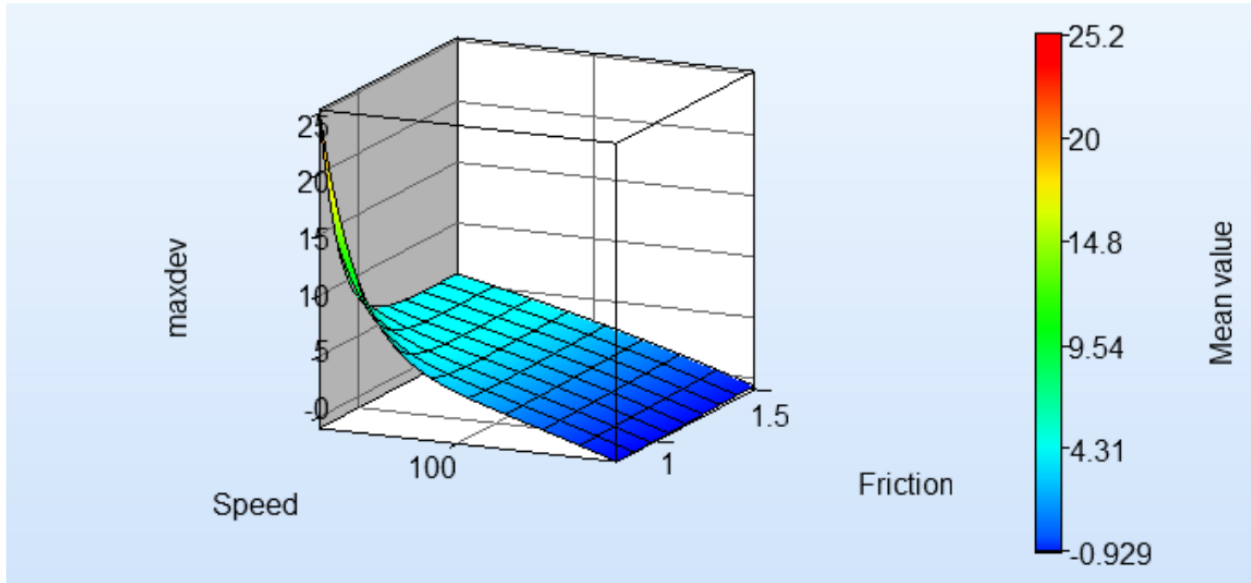


Figure 23. Surface Metamodel and Global sensitivity analysis: SUV, 3:1 straight road, 25 degree encroachment angle



Global Sensitivities Plot for maxdev
 Mean = 3.0124, Total variance = 6.38497, Noise variance = 5.67367e-005

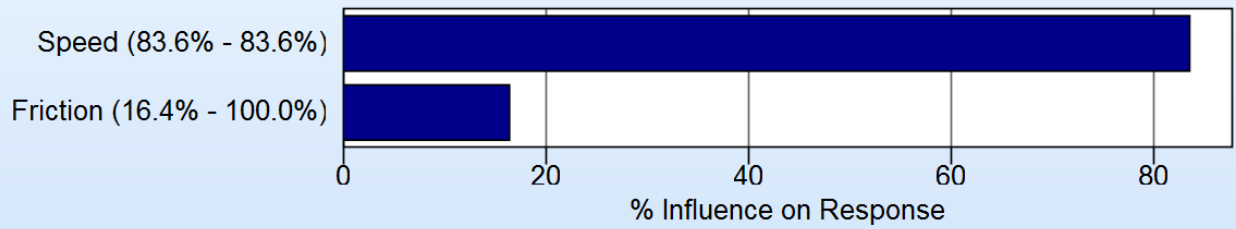
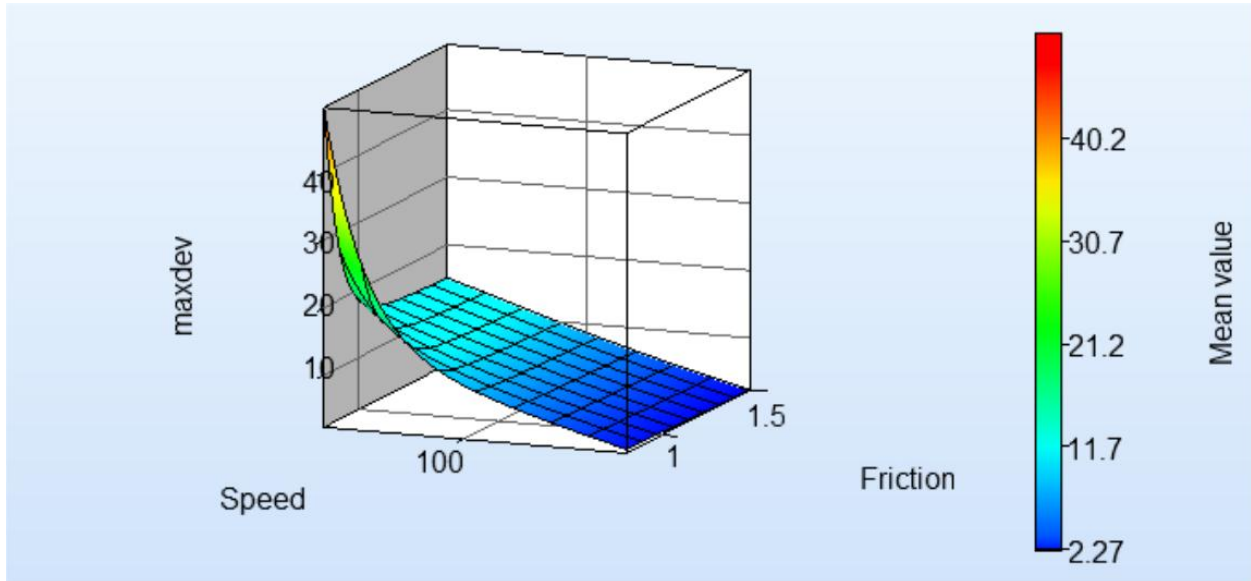


Figure 24. Surface Metamodel and Global sensitivity analysis: SUV, 4:1 curved road, 15 degree encroachment angle



Global Sensitivities Plot for maxdev
 Mean = 9.19585, Total variance = 23.0226, Noise variance = 0.242372

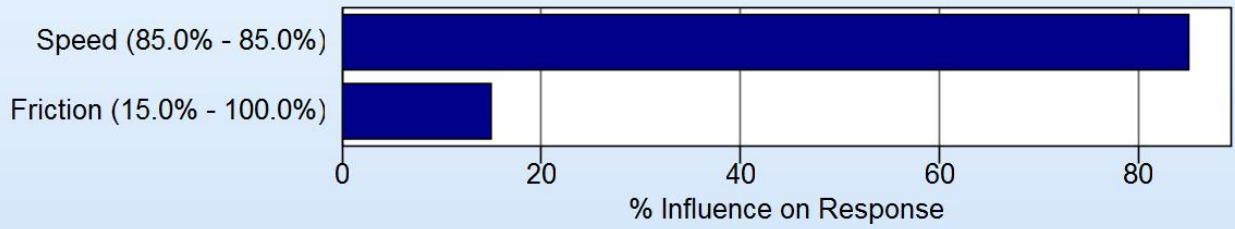
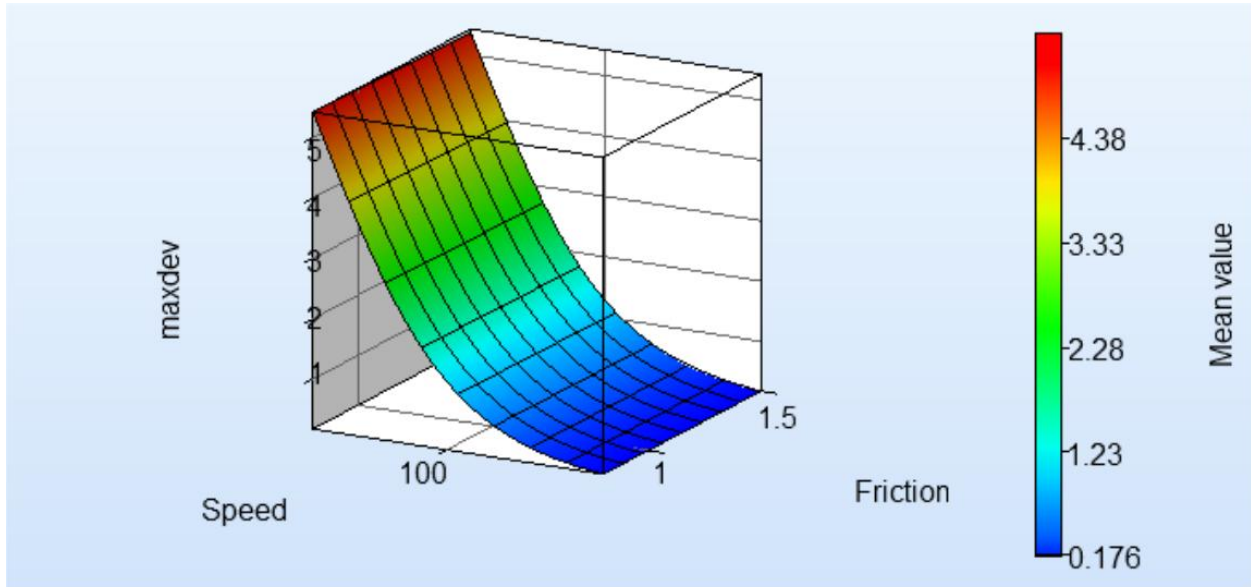


Figure 25. Surface Metamodel and Global sensitivity analysis: SUV. 4:1 curved road, 25 degree encroachment angle



Global Sensitivities Plot for maxdev
 Mean = 1.70025, Total variance = 2.29976, Noise variance = 7.0409e-010

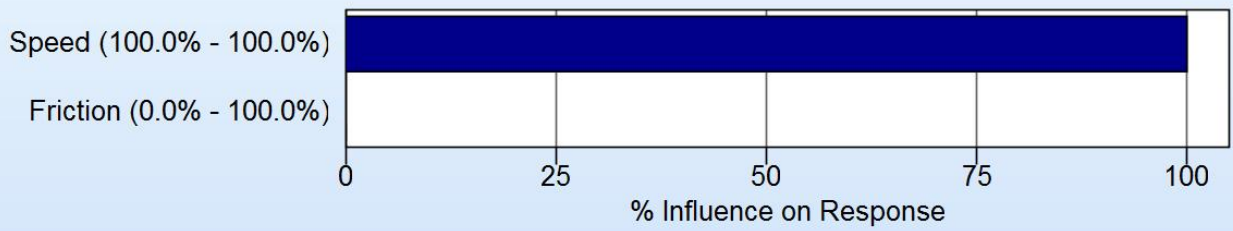
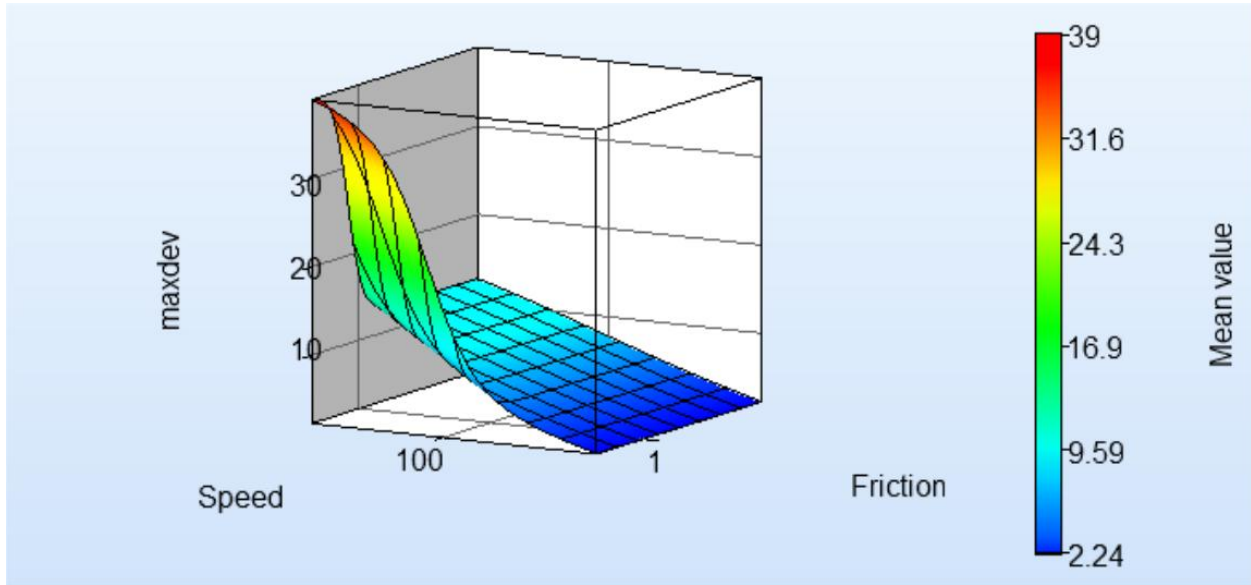


Figure 26. Surface Metamodel and Global sensitivity analysis: SUV, 4:1 straight road, 15 degree encroachment angle



Global Sensitivities Plot for maxdev
 Mean = 8.72252, Total variance = 39.5032, Noise variance = 0.00640533

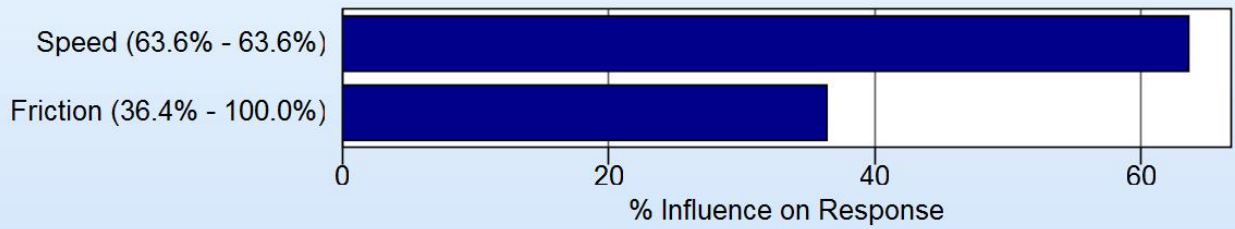
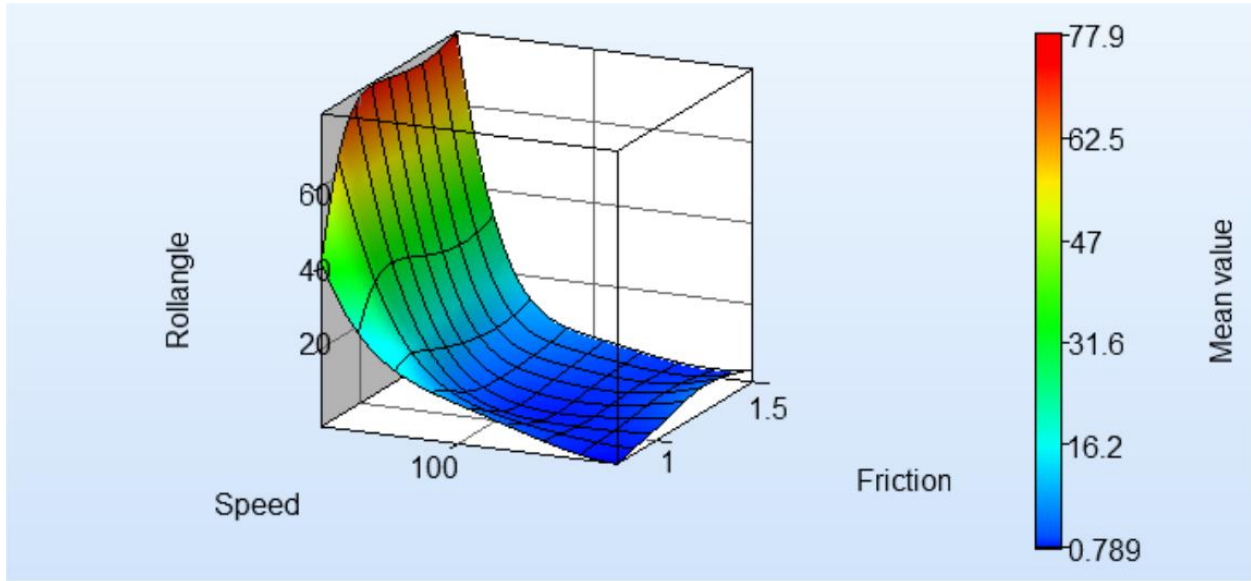


Figure 27. Surface Metamodel and Global sensitivity analysis: SUV, 4:1 straight road, 25 degree encroachment angle



Global Sensitivities Plot for Rollangle
 Mean = 13.0702, Total variance = 263.593, Noise variance = 24.2284

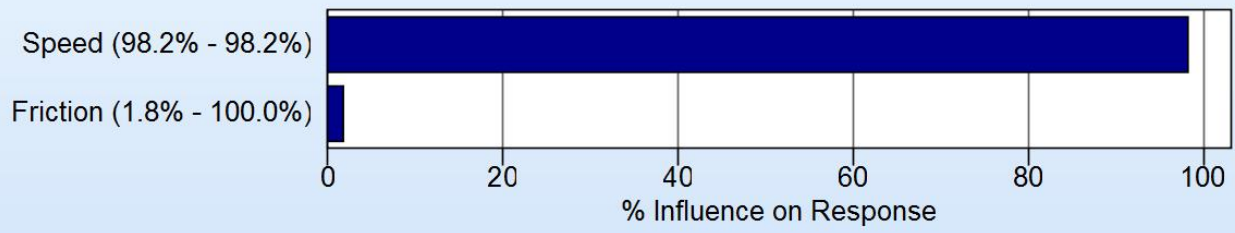
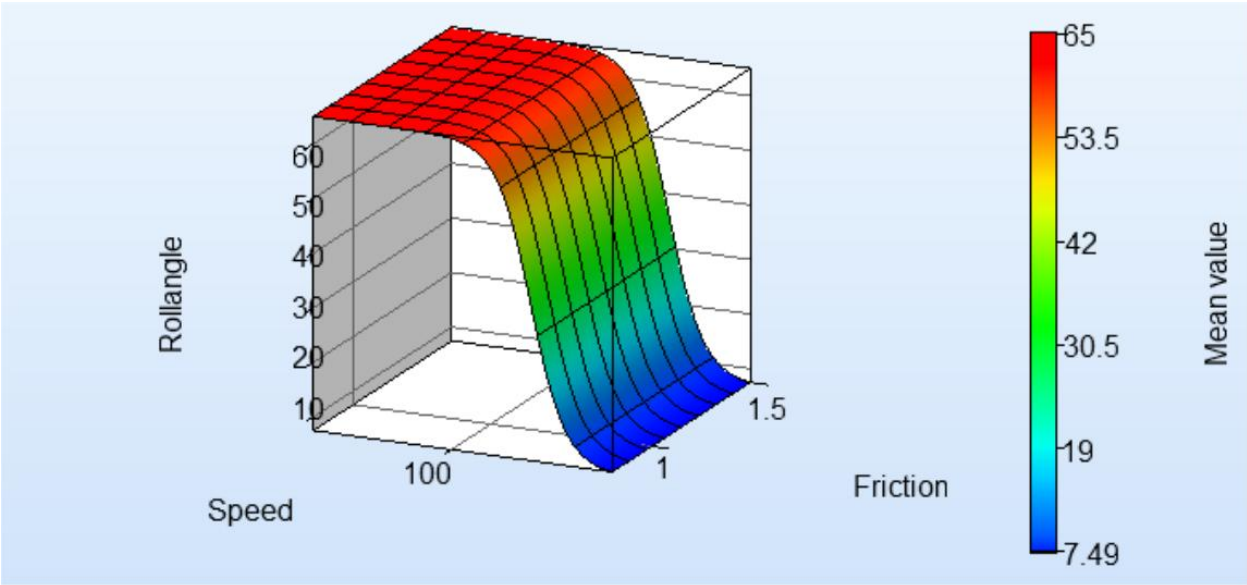


Figure 28. Surface Metamodel and Global sensitivity analysis: Class C hatchback, 3:1 curved road, 15 degree encroachment angle.



Global Sensitivities Plot for Rollangle
 Mean = 49.1902, Total variance = 472.949, Noise variance = 0.00012074

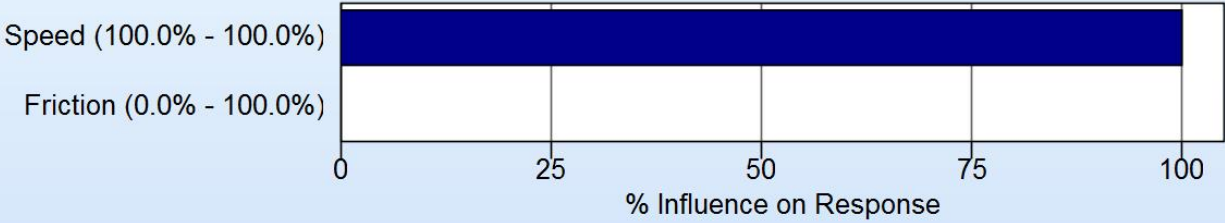
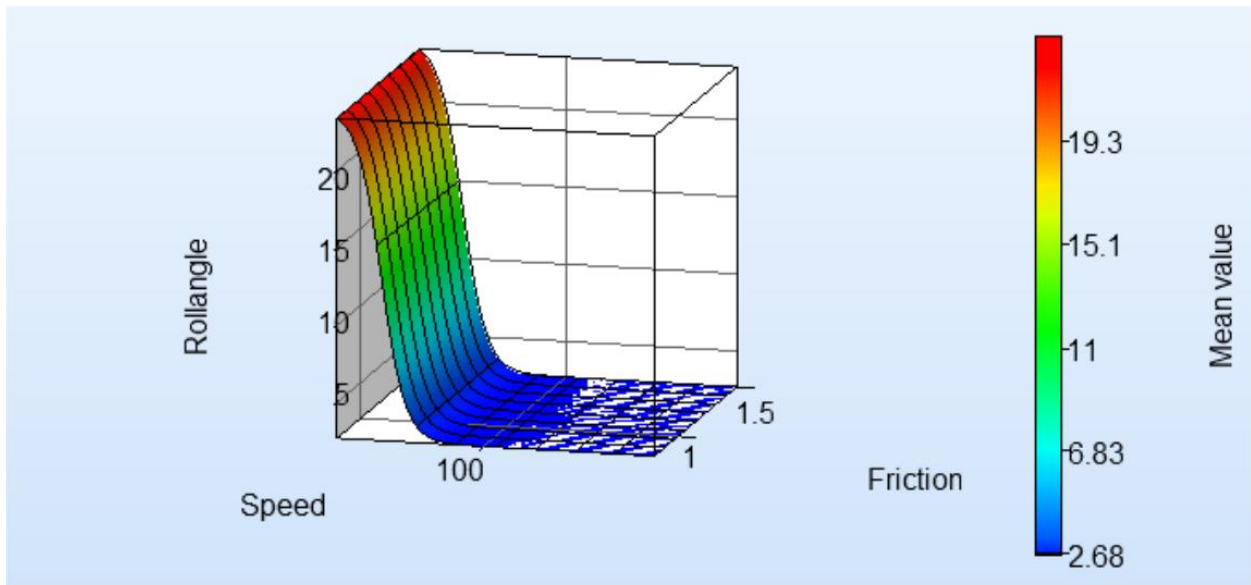


Figure 29. Surface Metamodel and Global sensitivity analysis: Class C hatchback, 3:1 curved road, 25 degree encroachment angle.



Global Sensitivities Plot for Rollangle
 Mean = 5.59782, Total variance = 37.1144, Noise variance = 0.000271373

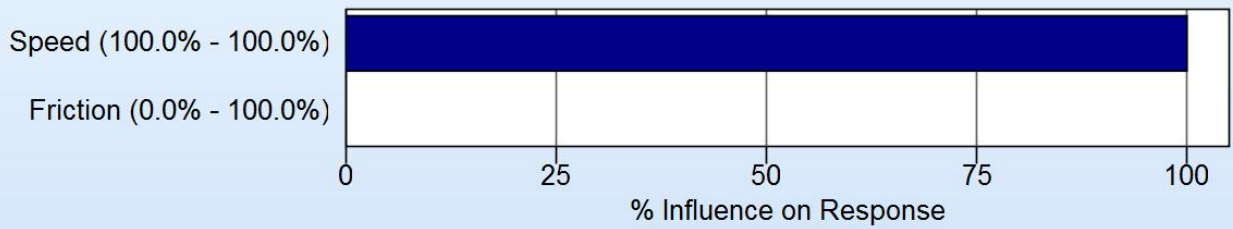
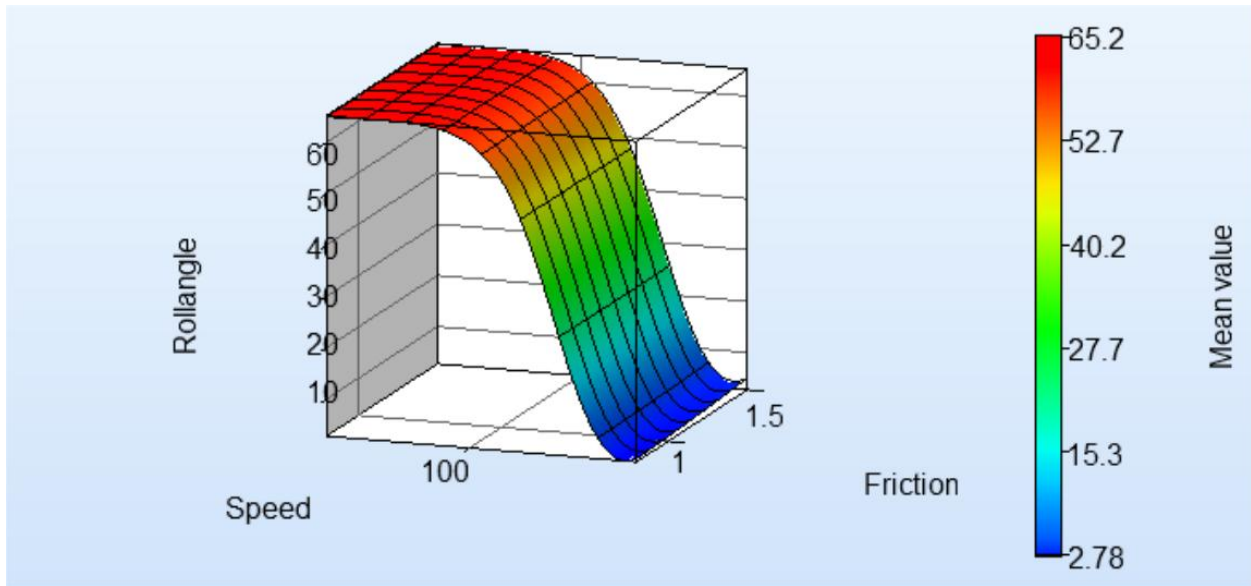


Figure 30 Surface Metamodel and Global sensitivity analysis: Class C hatchback, 3:1 straight road, 15 degree encroachment angle.



Global Sensitivities Plot for Rollangle
 Mean = 46.1454, Total variance = 531.37, Noise variance = 0.749899

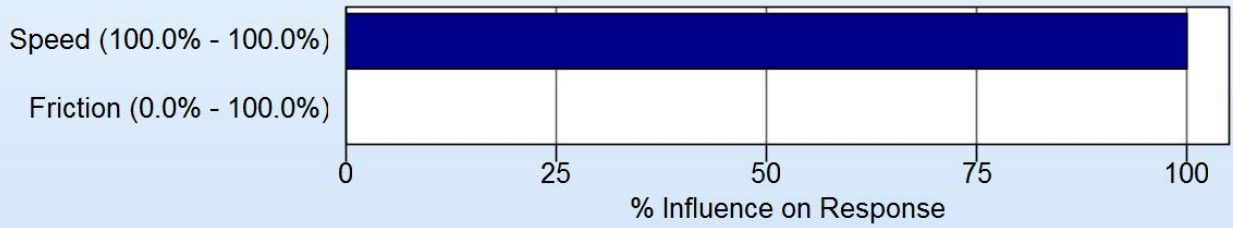
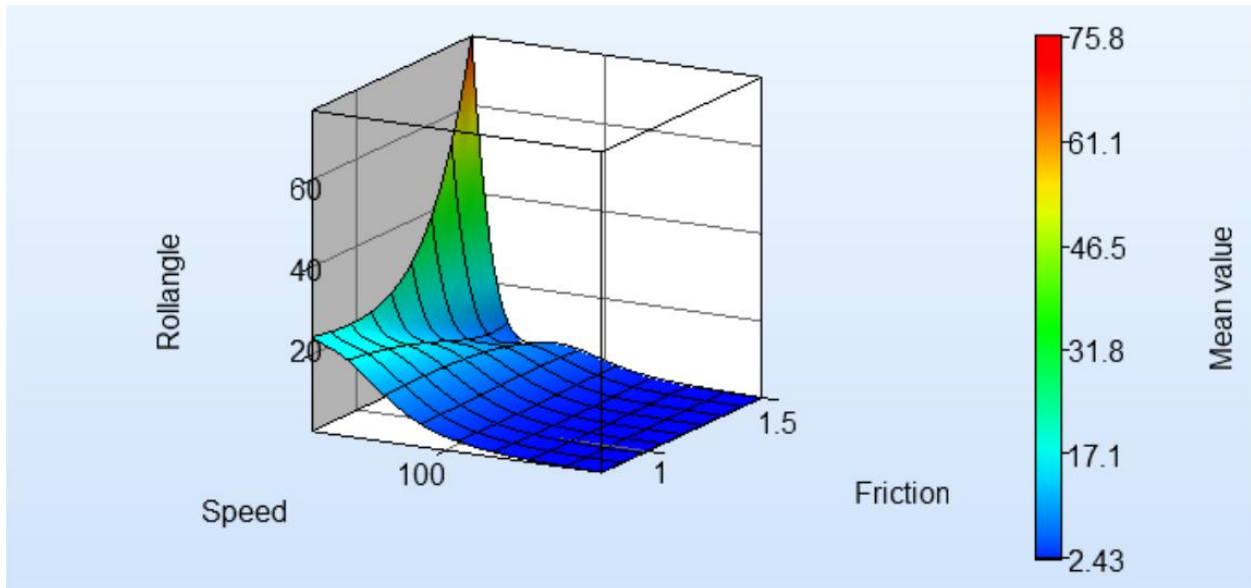


Figure 31 Surface Metamodel and Global sensitivity analysis: Class C hatchback, 3:1 straight road, 25 degree encroachment angle.



Global Sensitivities Plot for Rollangle
 Mean = 7.78885, Total variance = 44.6326, Noise variance = 0.864338

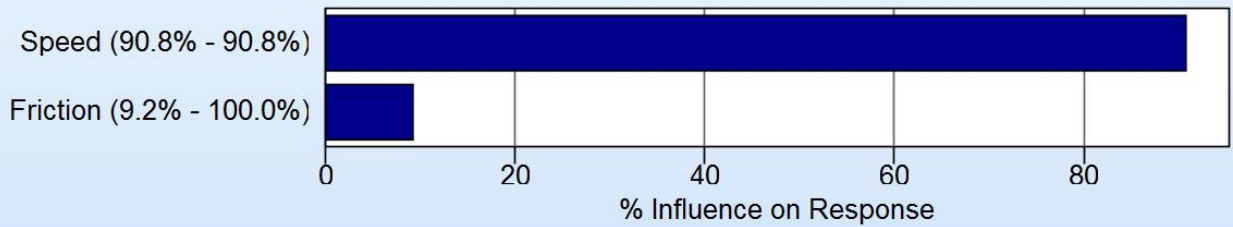
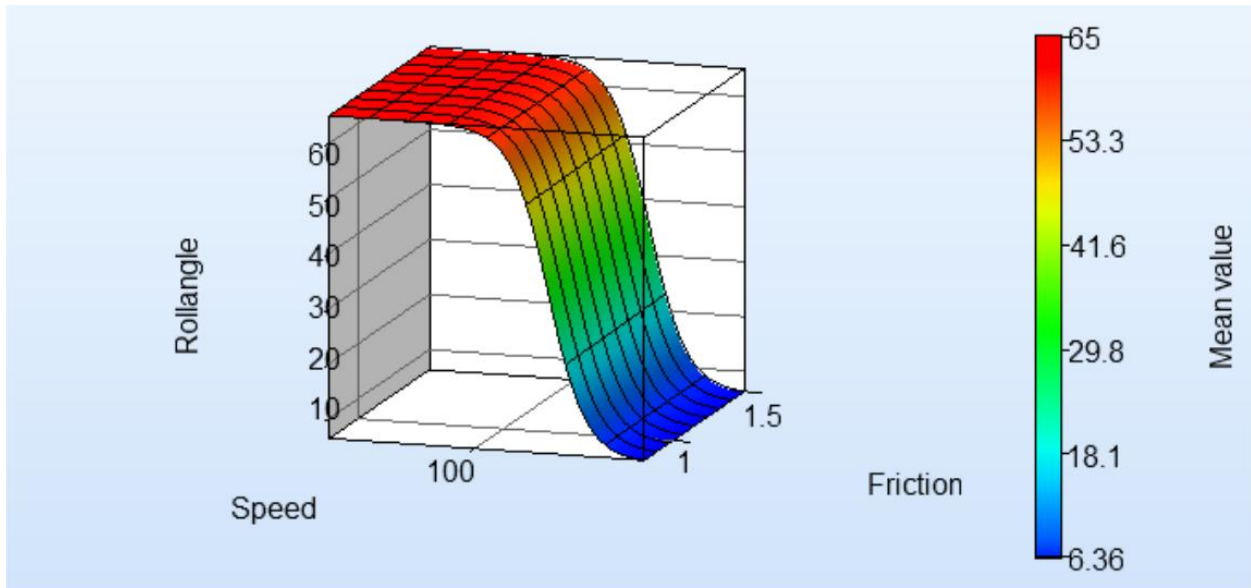


Figure 32 Surface Metamodel and Global sensitivity analysis: Class C hatchback, 4:1 curved road, 15 degree encroachment angle.



Global Sensitivities Plot for Rollangle
 Mean = 47.0493, Total variance = 529.844, Noise variance = 0.0141904

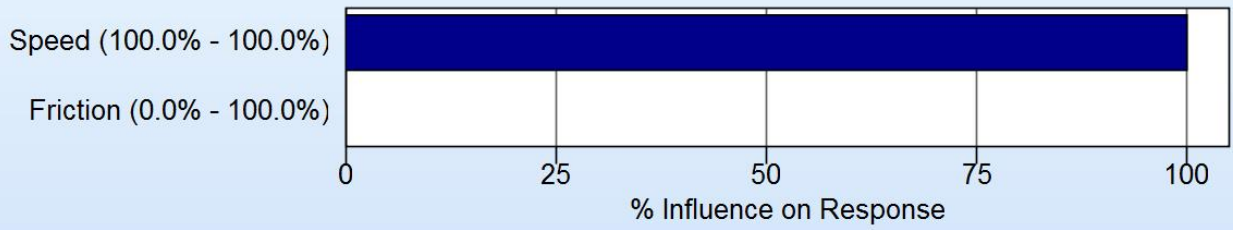
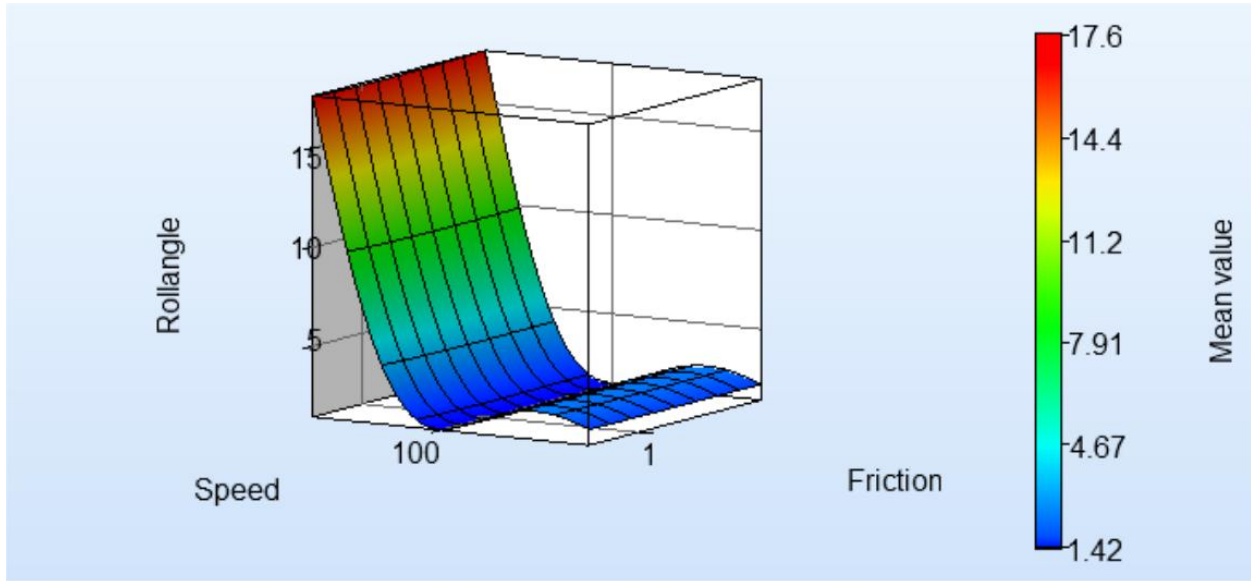


Figure 33 Surface Metamodel and Global sensitivity analysis: Class C hatchback, 4:1 curved road, 25 degree encroachment angle.



Global Sensitivities Plot for Rollangle
 Mean = 4.28253, Total variance = 15.4233, Noise variance = 0.108576

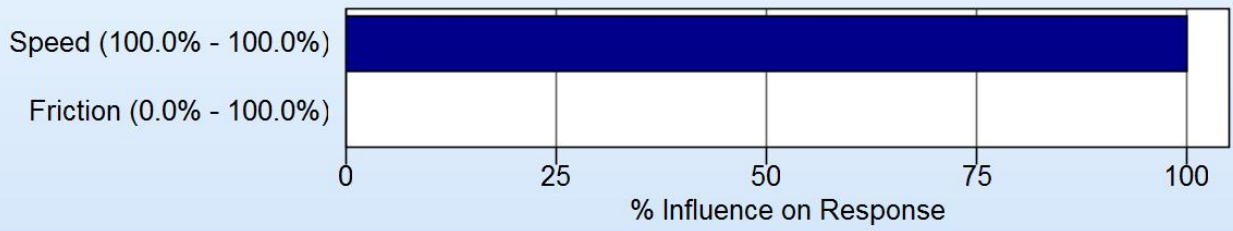
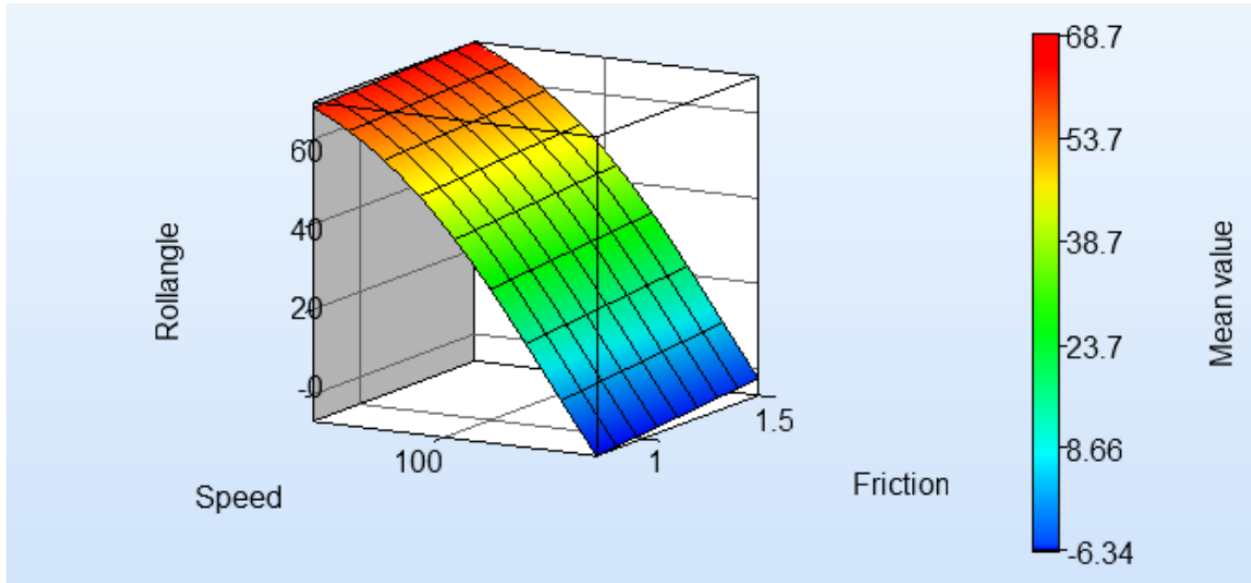


Figure 34 Surface Metamodel and Global sensitivity analysis: Class C hatchback, 4:1 straight road, 15 degree encroachment angle.



Global Sensitivities Plot for Rollangle

Mean = 38.2824, Total variance = 467.656, Noise variance = 0.00305406

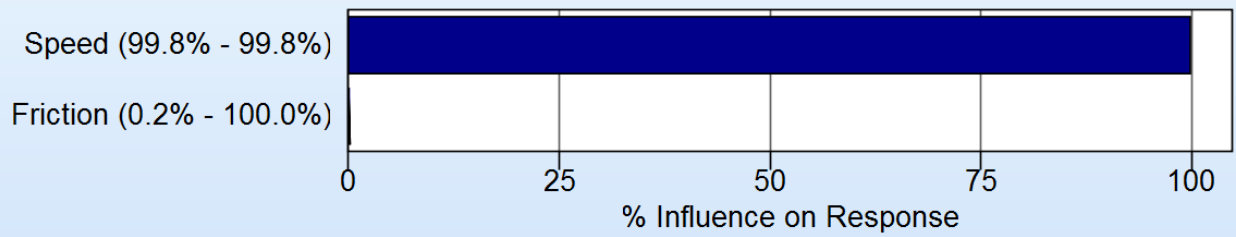
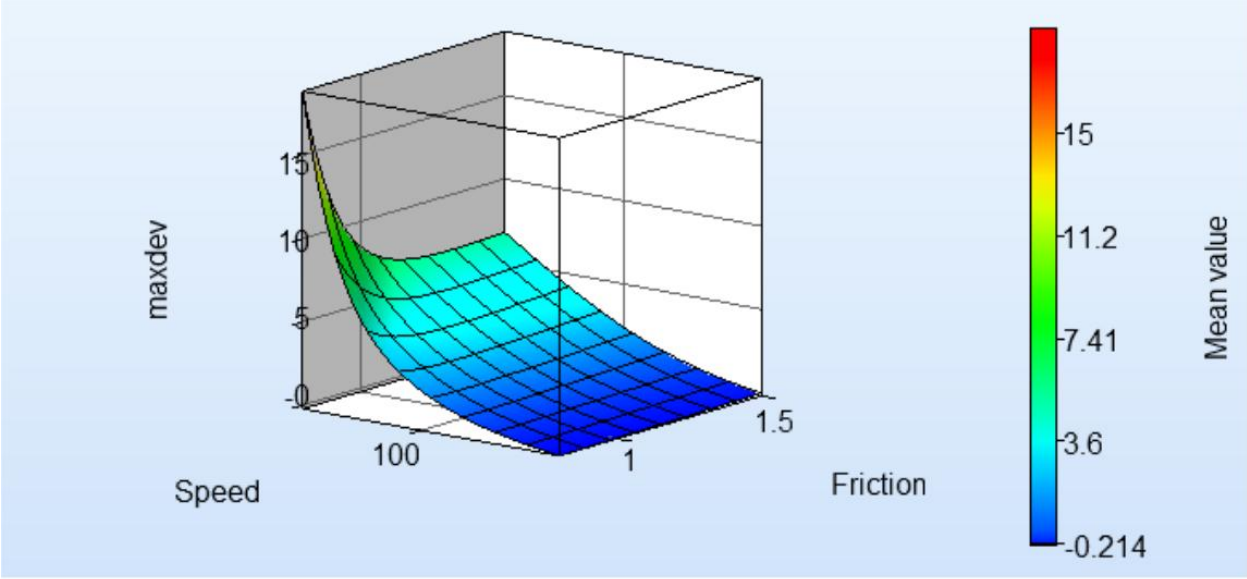


Figure 35 Surface Metamodel and Global sensitivity analysis: Class C hatchback, 4:1 straight road, 25 degree encroachment angle.



Global Sensitivities Plot for maxdev
 Mean = 2.56825, Total variance = 5.79408, Noise variance = 0.0107491

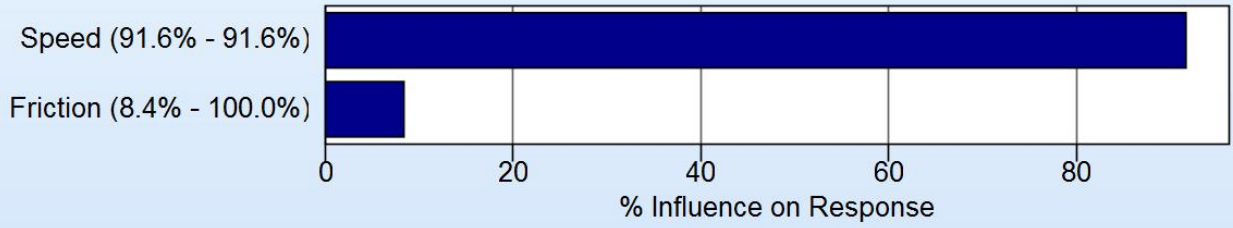
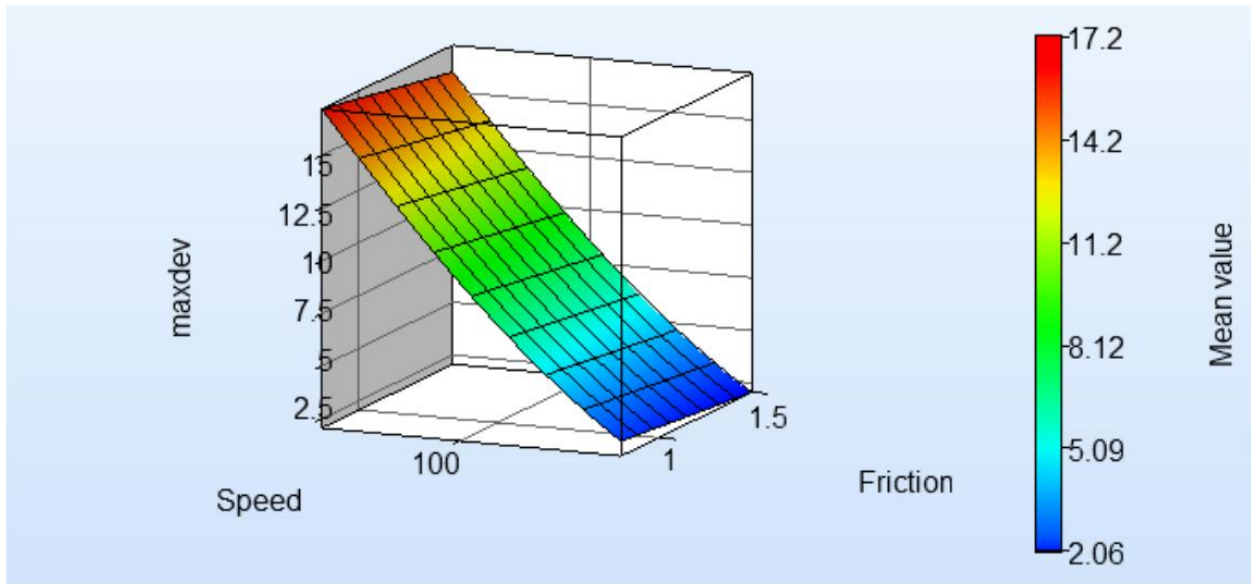


Figure 36 Surface Metamodel and Global sensitivity analysis: Class C hatchback, 3:1 curved road, 15 degree encroachment angle



Global Sensitivities Plot for maxdev
 Mean = 8.78146, Total variance = 16.9808, Noise variance = 0.000731363

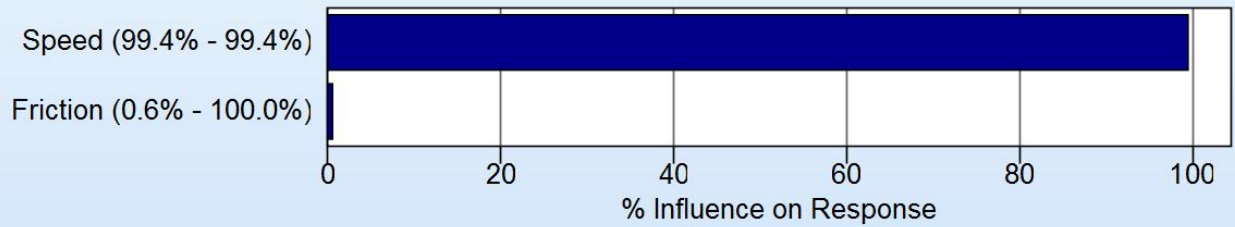
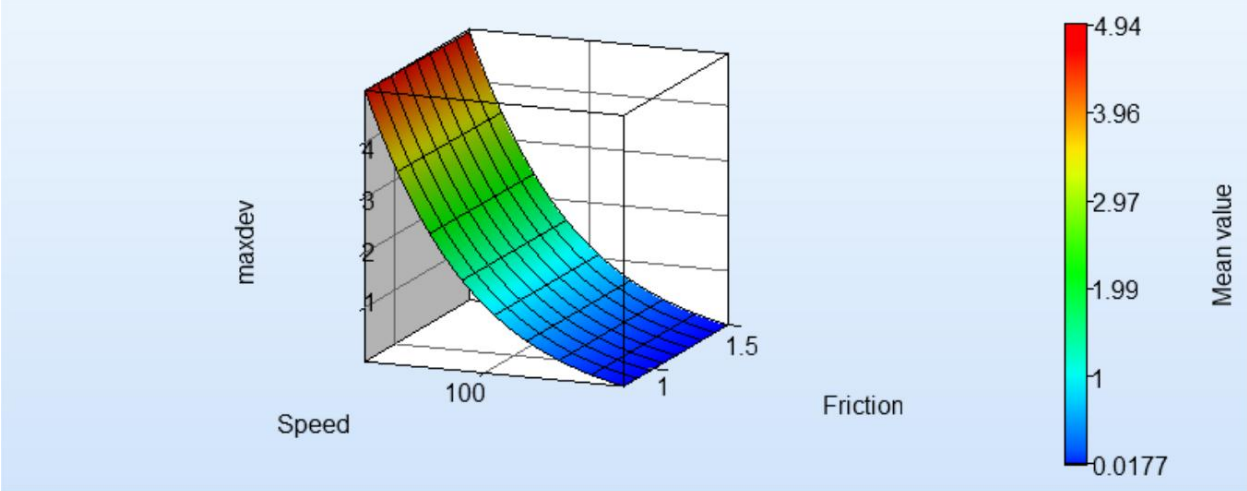


Figure 37 Surface Metamodel and Global sensitivity analysis: Class C hatchback, 3:1 curved road, 25 degree encroachment angle



Global Sensitivities Plot for maxdev
 Mean = 1.5156, Total variance = 1.83479, Noise variance = 3.99272e-006

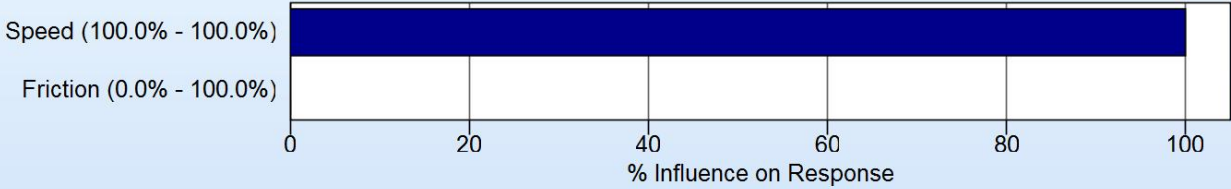
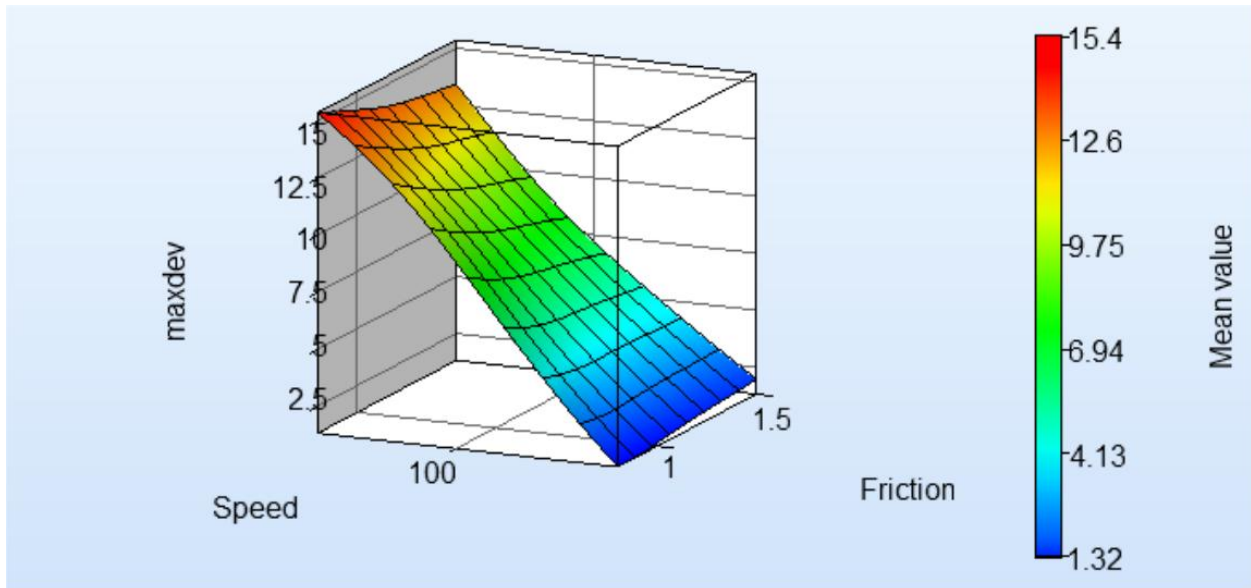


Figure 38 Surface Metamodel and Global sensitivity analysis: Class C hatchback. 3:1 straight road, 15 degree encroachment angle



Global Sensitivities Plot for maxdev
 Mean = 7.69091, Total variance = 13.776, Noise variance = 0.385372

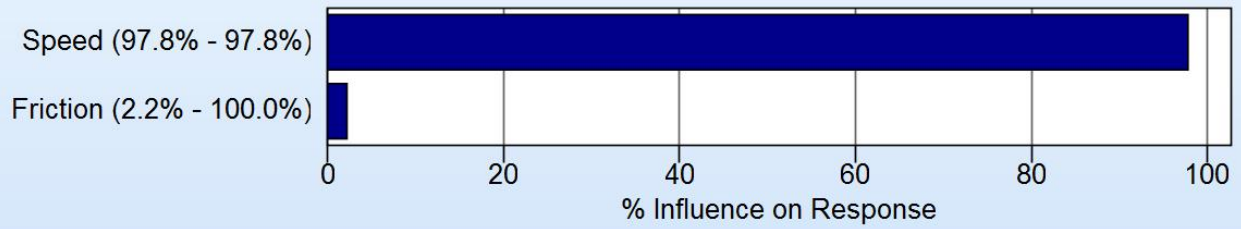
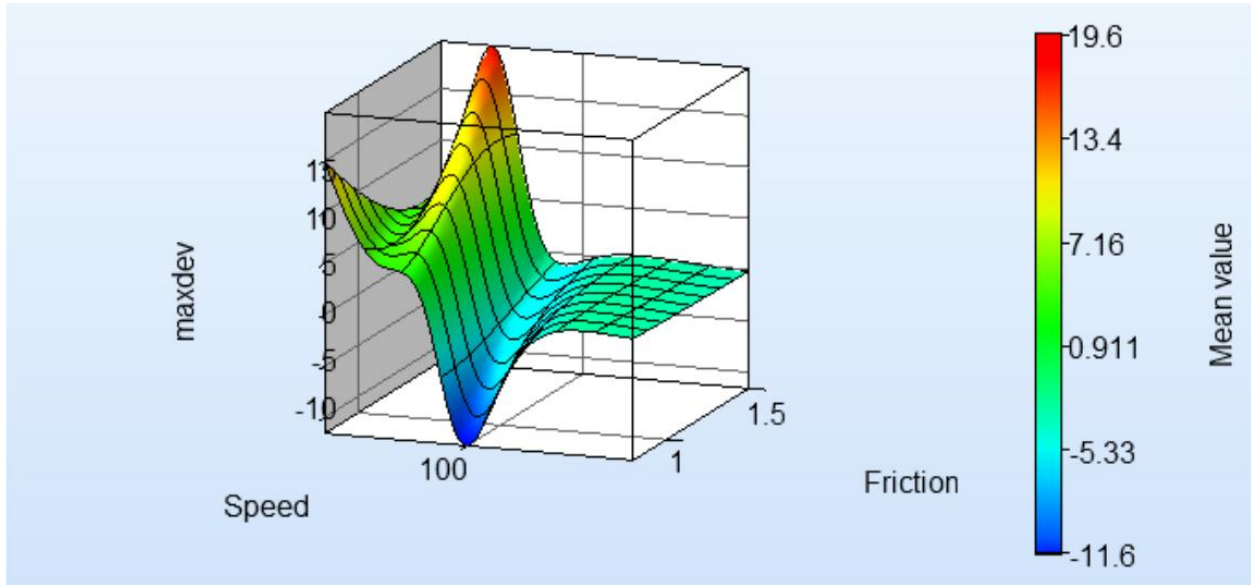


Figure 39 Surface Metamodel and Global sensitivity analysis: Class C hatchback, 3:1 straight road, 25 degree encroachment angle



Global Sensitivities Plot for maxdev
 Mean = 1.80496, Total variance = 26.3347, Noise variance = 1.66734

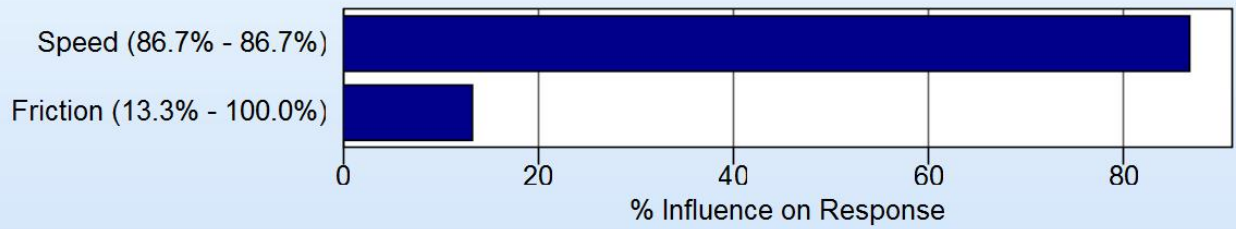
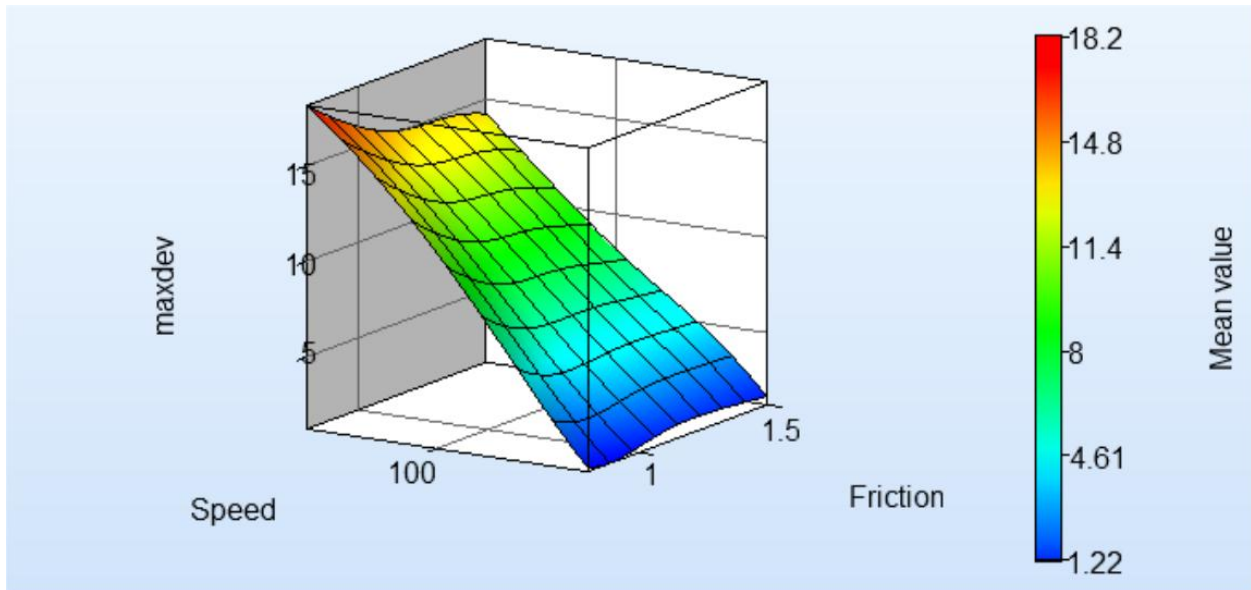


Figure 40 Surface Metamodel and Global sensitivity analysis: Class C hatchback, 4:1 curved road, 15 degree encroachment angle



Global Sensitivities Plot for maxdev
 Mean = 8.72107, Total variance = 17.0354, Noise variance = 0.155543

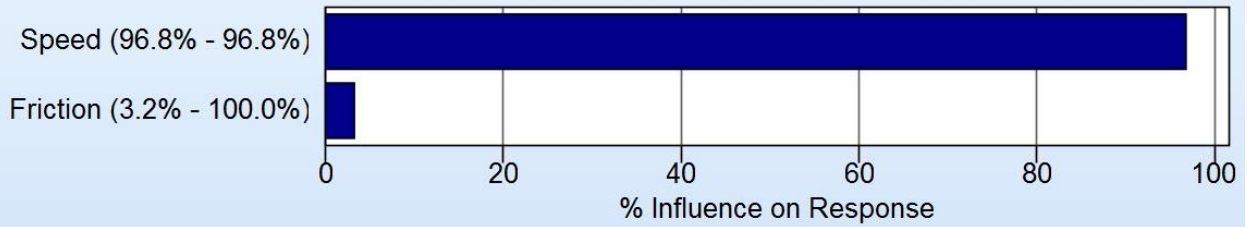
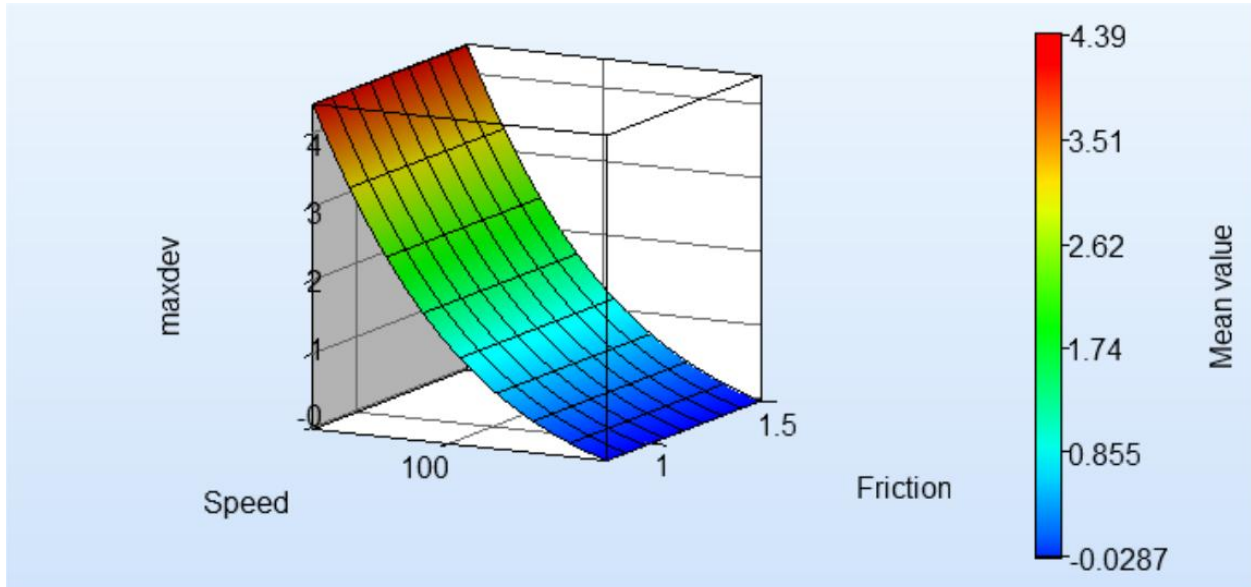


Figure 41 Surface Metamodel and Global sensitivity analysis: Class C hatchback, 4:1 curved road, 25 degree encroachment angle



Global Sensitivities Plot for maxdev
 Mean = 1.48164, Total variance = 1.55527, Noise variance = 6.73479e-008

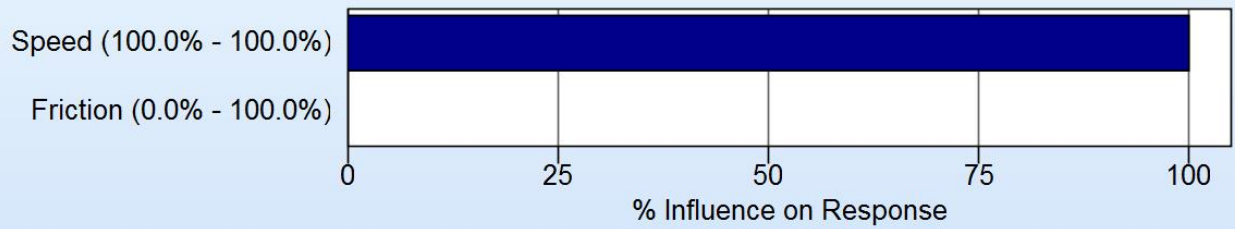
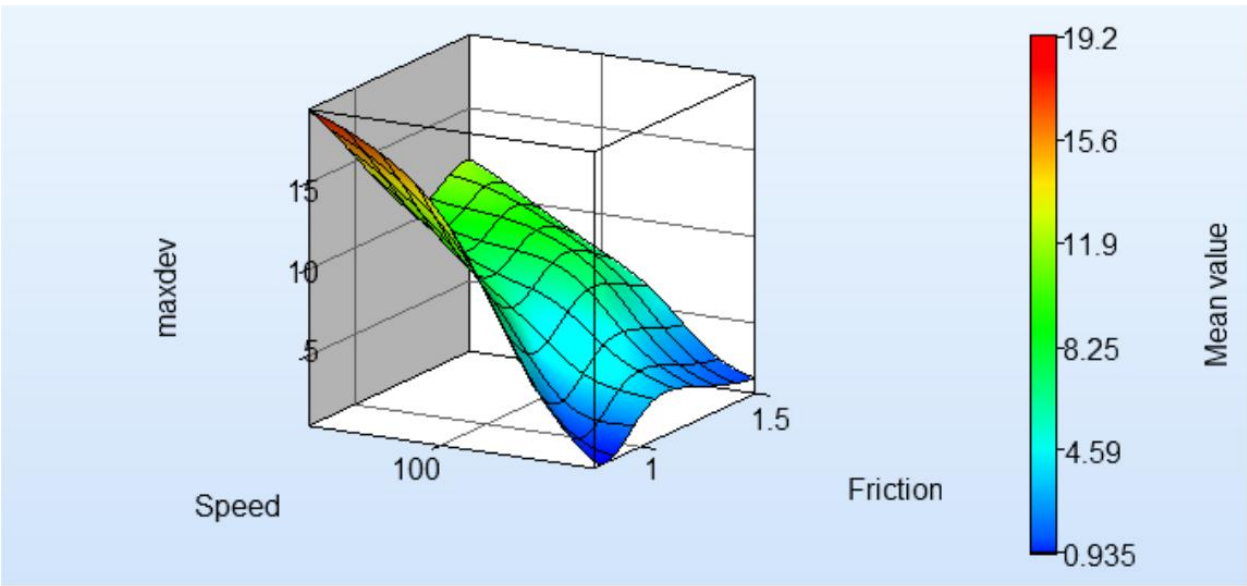


Figure 42 Surface Metamodel and Global sensitivity analysis: Class C hatchback, 4:1 straight road, 15 degree encroachment angle



Global Sensitivities Plot for maxdev
 Mean = 8.20645, Total variance = 16.0879, Noise variance = 4.58432

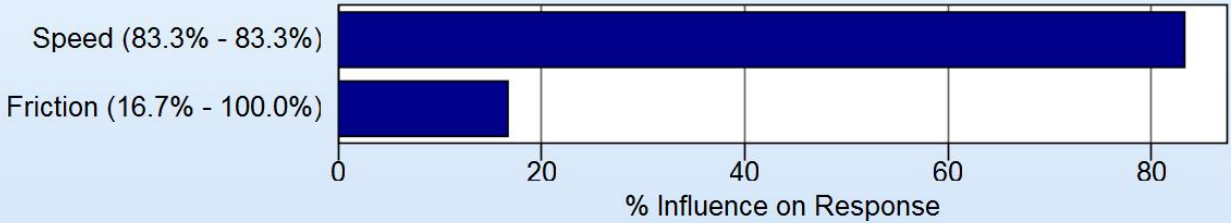


Figure 43 Surface Metamodel and Global sensitivity analysis: Class C hatchback, 4:1 straight road, 25 degree encroachment angle